



The May 2003 eruption of Anatahan volcano, Mariana Islands: Geochemical evolution of a silicic island-arc volcano

Jennifer A. Wade^{a,*}, Terry Plank^a, Robert J. Stern^b, Darren L. Tollstrup^c, James B. Gill^c,
Julie C. O’Leary^d, John M. Eiler^d, Richard B. Moore^e, Jon D. Woodhead^f,
Frank Trusdell^g, Tobias P. Fischer^h, David R. Hiltonⁱ

^aDepartment of Earth Sciences, Boston University, Boston, MA 02215, USA

^bGeosciences Department, University of Texas at Dallas, Richardson, TX 75083, USA

^cDepartment of Earth Sciences, University of California Santa Cruz, Santa Cruz, CA 95064, USA

^dDivision of Geological and Planetary Sciences, California Institute of Technology, Pasadena, CA 92215, USA

^eUnited States Geological Survey, Tucson, AZ 85719, USA

^fSchool of the Earth Sciences, The University of Melbourne, Victoria 3010, Australia

^gHawaiian Volcano Observatory, United States Geological Survey, Hawaii National Park, HI 96718, USA

^hDepartment of Earth and Planetary Sciences, University of New Mexico, Albuquerque, NM 87131, USA

ⁱFluids and Volatiles Laboratory, Scripps Institution of Oceanography, University of California San Diego, La Jolla, CA 92093, USA

Received 18 July 2004; accepted 28 November 2004

Abstract

The first historical eruption of Anatahan volcano began on May 10, 2003. Samples of tephra from early in the eruption were analyzed for major and trace elements, and Sr, Nd, Pb, Hf, and O isotopic compositions. The compositions of these tephra are compared with those of prehistoric samples of basalt and andesite, also newly reported here. The May 2003 eruptives are medium-K andesites with 59–63 wt.% SiO₂, and are otherwise homogeneous (varying less than 3% 2σ about the mean for 45 elements). Small, but systematic, chemical differences exist between dark (scoria) and light (pumice) fragments, which indicate fewer mafic and oxide phenocrysts in, and less degassing for, the pumice than scoria. The May 2003 magmas are nearly identical to other prehistoric eruptives from Anatahan. Nonetheless, Anatahan has erupted a wide range of compositions in the past, from basalt to dacite (49–66 wt.% SiO₂). The large proportion of lavas with silicic compositions at Anatahan (>59 wt.% SiO₂) is unique within the active Mariana Islands, which otherwise erupt a narrow range of basalts and basaltic andesites. The silicic compositions raise the question of whether they formed via crystal fractionation or crustal assimilation. The lack of ⁸⁷Sr/⁸⁶Sr variation with silica content, the MORB-like δ¹⁸O, and the incompatible behavior of Zr rule out assimilation of old crust, altered crust, or zircon-saturated crustal melts, respectively. Instead, the constancy of isotopic and trace element ratios, and the systematic variations in REE patterns are consistent with evolution by crystal fractionation of similar parental magmas. Thus, Anatahan is a type example of an island-arc volcano that erupts comagmatic basalts to dacites, with no evidence for

* Corresponding author. Tel.: +1 617 353 4085; fax: +1 617 353 3290.

E-mail address: jwade@bu.edu (J.A. Wade).

crustal assimilation. The parental magmas to Anatahan lie at the low $^{143}\text{Nd}/^{144}\text{Nd}$, Ba/La, and Sm/La end of the spectrum of magmas erupted in the Marianas arc, consistent with 1–3 wt.% addition of subducted sediment to the mantle source, or roughly one third of the sedimentary column. The high Th/La in Anatahan magmas is consistent with shallow loss of the top ~50 m of the sedimentary column during subduction.

© 2005 Elsevier B.V. All rights reserved.

Keywords: Anatahan volcano, Mariana Islands; geochemical evolution; island-arc volcano

1. Introduction

On May 10, 2003, Anatahan volcano awoke from its slumber and erupted for the first time in recorded history (see preface of this issue). An NSF-MARGINS rapid response team traveled to Anatahan on May 18–21, 2003 to collect samples from the recent eruption (Fig. 1; Trusdell et al., 2005—this issue). We report here the geochemical composition of these samples, focusing on two themes: (1) the origin of silicic magmas in an island-arc volcano, and (2) the subducted sediment contribution to Anatahan magmas.

Prior published work reported basalts (with ~50 wt.% SiO_2) to dacites (>63 wt.% SiO_2) on Anatahan (Woodhead, 1989; Woodhead et al., 2001). Such silicic compositions are unusual for volcanoes of the Mariana Islands, which erupt largely basalts and basaltic andesites (Stern et al., 2003). Thus, Anatahan provides the best opportunity for addressing questions of magma evolution in this classic island arc, specifically the relative roles of fractional crystallization and crustal assimilation (Davidson, 1987; Hildreth and Moorbath, 1988; Woodhead, 1989).

The incorporation of subducted seafloor sediments into the sub-arc mantle greatly affects the geochemical composition of arc eruptives (Gill, 1981; Tera et al., 1986; Plank and Langmuir, 1993). Sediments impart chemical signatures such as negative Ce anomalies, Nb anomalies, and high $^{207}\text{Pb}/^{204}\text{Pb}$, which, in the Marianas, can vary from island to island (Dixon and Batiza, 1979; Elliott et al., 1997; Hole et al., 1984; Lee et al., 1995; Woodhead, 1988). Until now, there have been too few high quality isotopic or trace element data to treat this aspect of Anatahan.

1.1. The new eruptives

The MARGINS team retrieved a total of 18 samples from two sites on Anatahan, one on a

meadow on the east side of the island, and the other on a beach on the west side near an abandoned village (Fig. 1; Table 1). On the basis of subsequent correlation to the stratigraphy described in Trusdell et al. (2005—this issue), 12 of the samples were determined to be from the recent eruption, all of which were taken from the three West Beach sampling sites (Fig. 2). Given the timing of collection (May 19–21, 2003), all juvenile samples collected by the MARGINS team derive from the initial phases (May 10–18, 2003) of the eruption, and correlate with the lower three units (basal scoria, red ash, and main scoria) defined by Trusdell et al. (2005—this issue). For this reason, we refer to these samples henceforth as May 03 eruptives. Another relatively large eruption, which occurred on June 14, was dominated by steam and coarse ash, and is most likely represented by blocks embedded in an upper phreatomagmatic deposit (Trusdell et al., 2005—this issue). We also analyzed an additional sample of the “main scoria” collected in September 2003 (Reagan et al., 2005—this issue). The eruption continues as of this writing (June 2004). For more details on the nature of the continuing eruption, see Trusdell et al. (2005—this issue). Pallister et al. (2005—this issue) report detailed petrographic descriptions, and analyses of glasses, phenocrysts, and melt inclusions, focusing on the recent eruption. de Moor et al. (2005—this issue) report volatile and major element data on the same May 03 MARGINS samples studied here.

While collecting tephra from the May eruption, the MARGINS team also gathered lavas and bombs from prehistoric eruptions for comparative purposes (these are all from the eastern site; Fig. 1). In April 2004, several of the authors returned to Anatahan to collect six more prehistoric samples, in an attempt to sample more mafic material. The samples were collected from a beach and surrounding cliffs and valley on the southwest side of the island, as well as a

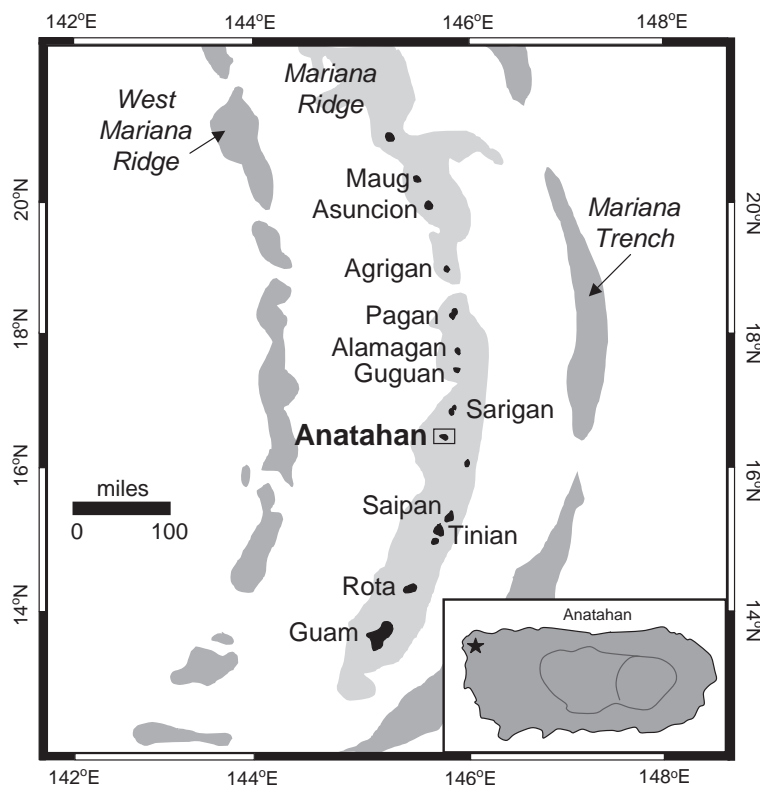


Fig. 1. Location map of the Mariana islands. Star on the inset map of Anatahan island shows the West Beach site sampled in May 2003 by the MARGINS team.

second beach cliff on the west side. We report new analyses of these samples to provide a self-consistent dataset with which to compare the May 03 samples. We also report data for 11 samples collected during USGS field campaigns in the 1990s, which further extend the range of compositions previously reported (Moore et al., 1991, 1993; Rowland et al., 2005—this issue). Finally, we include new analyses of the prehistoric Anatahan samples reported in Woodhead and Fraser (1985), Woodhead (1988, 1989), and Woodhead et al. (2001).

2. Methods

2.1. Sample preparation of MARGINS samples collected in May 2003

The MARGINS samples were prepared at Scripps Institution of Oceanography. Each sample

was broken with a hammer and chisel to collect an inner, unweathered section. Those sections were sonicated in ~10% HCl for 15 min, then dried at 100 °F. Samples were pulverized using an alumina–ceramic shatter box. Two of the six samples collected in April 2004 are coarse scoria, two are ash and lapilli, and two are bombs. The bombs were broken with a hammer to collect inner fresh pieces, then all samples were rinsed in MilliQ water and dried before being pulverized in an alumina–ceramic ball mill. Major elements, trace elements, and Sr, Nd, Pb, and Hf isotopic ratios were determined on different aliquots of these powders (Tables 1, 2, and 5). Oxygen isotopic analyses were determined on hand-picked groundmass separates from different splits of the MARGINS samples (see Section 2.5 and Table 6).

Many of the samples were collected in pairs, based on color and buoyancy differences. Pumice fragments are lighter in color and float in water, while scoria

Table 1

Major and trace element analyses for Anatahan samples erupted and collected in May 2003 by the MARGINS team

Sample name	Anat5	Anat6-p	Anat6-s	Anat7-p	Anat7-s	Anat8-p	Anat8-s	Anat10-p	Anat10-s	Anat11	Anat12-p	Anat12-s	FTM-03-20C
Location	WB-Sec1a	WB-Sec1b	WB-Sec1b	WB-Sec1cd	WB-Sec1cd	WB-Sec1e	WB-Sec1e	WB-Sec2	WB-Sec2	WB-Sec3d	WB-Sec3a	WB-Sec3a	EC-5
Sample type	Fine ash	Lapilli (P)	Lapilli (S)	Coarse ash (P)	Coarse ash (S)	Scoria (P)	Scoria (S)	Scoria (P)	Scoria (S)	Scoria (S)	Fine ash (S)	Scoria (P)	Scoria (S)
Rock type	Andesite	Andesite	Andesite	Dacite	Andesite	Andesite	Andesite	Andesite	Andesite	Andesite	Andesite	Andesite	Andesite
SiO ₂	59.77	61.0 ^a	60.37	63.0 ^a	59.74	61.0 ^a	59.9 ^a	59.7 ^a	59.75	58.85	59.89	60.97	59.83
TiO ₂	0.879	0.861	0.891	0.798	0.895	0.863	0.893	0.850	0.904	0.859	0.859	0.881	0.927
Al ₂ O ₃	16.37	15.58	16.07	15.12	15.81	15.59	15.72	18.50	15.62	16.33	16.32	15.98	15.35
Fe ₂ O ₃ *	9.39	9.16	9.28	8.52	9.35	9.18	9.51	8.83	9.39	9.22	8.61	8.77	9.34
MnO	0.208	0.209	0.213	0.193	0.215	0.209	0.213	0.207	0.218	0.201	0.220	0.220	0.224
MgO	2.17	2.03	2.19	1.97	2.12	2.05	2.16	2.02	2.15	2.16	2.05	2.07	2.12
CaO	6.04	5.63	6.02	5.31	5.96	5.61	5.90	5.61	5.97	6.08	5.78	5.97	5.89
Na ₂ O	3.82	3.95	3.95	3.68	3.82	3.93	4.07	3.73	3.96	3.75	4.13	4.06	4.02
K ₂ O	1.28	1.26	1.37	1.17	1.30	1.28	1.26	1.29	1.36	1.27	1.43	1.41	1.42
P ₂ O ₅	0.281	0.320	0.283	0.288	0.286	0.297	0.321	0.277	0.303	0.266	0.279	0.272	0.280
Total	100.2	100.0	100.6	100.0	99.5	100.0	100.0	101.0	99.6	99.0	99.6	100.6	99.4
LOI	nd	nd	-0.07	nd	0.06	nd	nd	0.49	0.18	1.04	0.09	-0.15	0.16
Li	10.8	12.2	11.1	11.4	11.5	12.0	11.5	11.8	11.9	10.8	12.2	11.5	12.9
Be	0.933	0.978	0.976	0.918	0.976	0.997	0.943	0.946	1.00	0.915	0.975	0.962	1.02
Sc	26.8	26.8	28.1	24.6	27.1	26.6	28.0	26.6	28.5	27.0	28.0	27.3	28.8
V	139	124	138	124	134	124	139	125	134	136	125	132	124
Cr	1	0	1	1	1	4	0	10	0	1	0	0	5
Co	23.1	20.6	22.0	20.4	20.9	20.1	20.3	18.9	19.6	20.2	20.4	22.7	19.0
Ni	11.48	9.29	10.63	7.92	8.92	7.16	6.83	5.05	2.77	6.65	5.37	7.74	2.81
Cu	66	62	58	56	62	60	60	60	61	67	61	59	63
Zn	106	111	110	100	109	108	109	108	112	104	112	108	114
Rb	26.0	27.7	27.3	25.0	27.5	27.1	27.0	26.7	27.6	25.4	27.8	26.8	28.8
Sr	360	362	369	332	367	356	368	356	370	365	366	363	380
Y	36.2	38.8	37.6	34.8	38.0	38.3	38.6	37.2	39.1	36.1	39.1	37.9	40.9
Zr	110	120	116	110	117	117	117	115	116	107	116	112	122
Nb	2.53	2.64	2.64	2.71	2.62	2.90	2.81	2.80	2.83	2.66	2.76	2.91	2.82
Cs	0.650	0.672	0.643	0.604	0.674	0.659	0.645	0.655	0.698	0.672	0.703	0.673	0.746
Ba	376	406	390	367	394	398	392	406	402	379	407	397	427
La	11.2	12.1	11.6	11.0	11.7	12.0	11.8	11.6	12.4	11.7	12.6	12.2	12.8
Ce	24.5	26.7	25.5	24.1	25.8	26.4	26.2	25.5	26.2	24.7	26.8	25.9	28.1
Pr	3.71	3.99	3.86	3.64	3.89	3.99	3.92	3.85	3.88	3.62	3.94	3.80	4.24
Nd	17.0	18.5	17.8	16.9	18.0	18.3	18.2	17.7	18.1	17.0	18.5	17.9	19.0
Sm	4.73	5.07	4.92	4.66	4.94	5.01	5.02	4.88	4.98	4.72	5.06	4.90	5.16
Eu	1.55	1.65	1.61	1.49	1.62	1.61	1.62	1.60	1.64	1.53	1.65	1.62	1.64
Gd	5.49	5.99	5.81	5.40	5.80	5.92	5.90	5.70	6.09	5.69	6.23	6.03	6.17
Tb	0.93	1.00	0.97	0.92	0.98	0.99	1.00	0.97	1.04	0.96	1.05	1.02	1.05
Dy	5.87	6.36	6.16	5.75	6.21	6.25	6.30	6.16	6.52	6.02	6.58	6.45	6.56
Ho	1.27	1.37	1.33	1.24	1.33	1.34	1.34	1.32	1.38	1.29	1.41	1.37	1.42
Er	3.54	3.80	3.73	3.46	3.74	3.73	3.76	3.67	3.94	3.70	4.02	3.89	4.02
Yb	3.54	3.80	3.71	3.45	3.73	3.73	3.77	3.64	3.88	3.59	3.92	3.89	4.04
Lu	0.554	0.593	0.583	0.538	0.582	0.585	0.586	0.569	0.610	0.587	0.634	0.624	0.634
Hf	2.96	3.17	3.07	2.94	3.11	3.18	3.14	3.07	3.08	2.84	3.15	3.12	3.36
Ta	0.189	0.204	0.198	0.186	0.200	0.201	0.200	0.196	0.201	0.188	0.201	0.199	0.202
Pb	5.08	4.99	4.79	4.59	4.94	4.98	4.90	4.89	4.89	4.80	5.08	4.96	5.15
Th	1.69	1.82	1.75	1.66	1.77	1.79	1.79	1.75	1.78	1.65	1.84	1.85	1.88
U	0.656	0.727	0.696	0.660	0.697	0.710	0.699	0.742	0.696	0.649	0.716	0.704	0.740

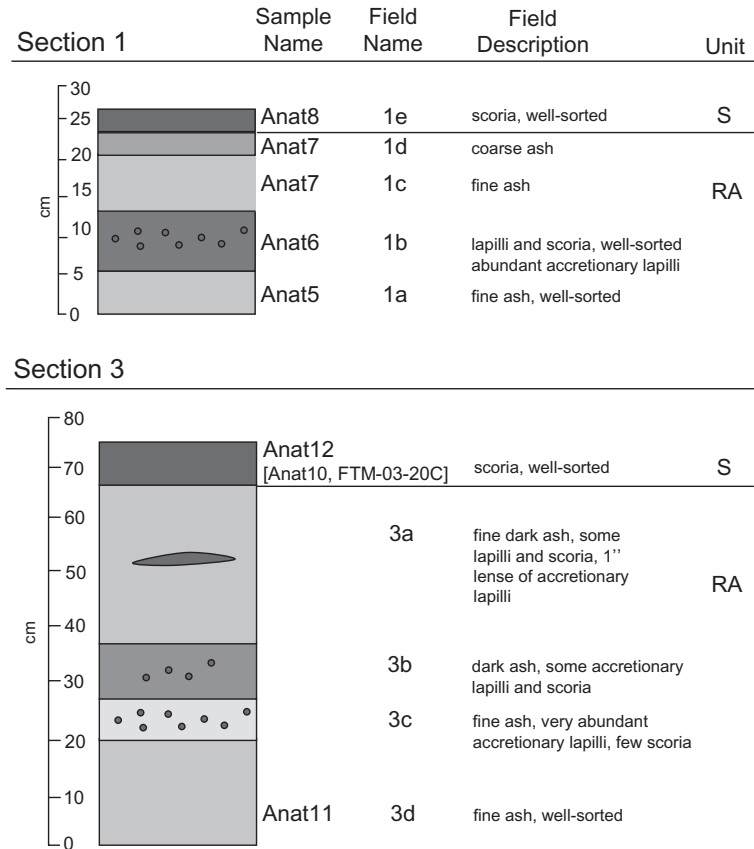


Fig. 2. Stratigraphic columns for Sections 1 and 3 of the May 2003 eruption of Anatahan, as reported by the MARGINS sampling team. Both sections are from the West Beach Site (see Fig. 1) and include material primarily from the initial blast of May 10, 2003 (Pallister et al., 2005—this issue). Sample names in brackets are also from the main scoria, but were collected from other locations (see Table 1). “S” (scoria) and “RA” (red ash) refer to unit names from Trusdell et al. (2005—this issue).

fragments are darker and denser. Pallister et al. (2005—this issue) noted that both the light and dark phases may occur within the same lapilli, with dark regions in the core and lighter regions in lapilli margins. Despite these differences, scoria and pumice fractions from each sample have very similar chemical compositions (see below and Pallister et al., 2005—this issue). de Moor et al. (2005—this issue) thus

report major element compositions for bulk samples from each site. On the other hand, because the goal of this study was to explore geochemical variations, we analyzed separate scoria and pumice fractions for trace element and isotopic analyses (see -S and -P samples in Table 1). Thus, although the original scope of our project was geochemical (trace elements and isotopes), we also measured major element abundan-

Notes to Table 1:

Major elements were acquired by ICP-AES and trace elements by ICP-MS at Boston University. Sample type refers to macroscopic description; some samples are further divided into pumice (P) and darker scoria (S) separates. Total Fe reported as Fe₂O₃*. LOI=loss on ignition; nd=not determined. WB=samples collected near the West Beach sampling site (N16°21'42.9", E145°38'0.35"). EC-5 is the site of an electronic distance network point on Anatahan, where this sample was taken (N16°20'46.6", E145°39'55.55"; Pallister et al., 2005—this issue; Trusdell et al., 2005—this issue).

^a SiO₂ calculated by difference.

Table 2

Major and trace element analyses for pre-historic Anatahan samples collected by two MARGINS teams in May 2003 and April 2004

Sample name	Collected in May						Collected in April					
	Anat1	Anat2	Anat3	Anat4-p	Anat4-s	Anat9	04-Anat-01	04-Anat-02	04-Anat-03	04-Anat-04	Anat-26-01	Anat-26-02
Location	EM	EM	EM	EM	EM	WB	SW	SW valley	W cliff 1	W cliff 2	SW	SW
Sample type	Bomb	Lava	Lava with phenos	Scoria (P)	Scoria (S)	Lava	Scoria	Bomb	Bomb	Scoria	Ash/lapilli	Ash/lapilli
Rock type	Andesite	Dacite	Basalt	Dacite	Andesite	Dacite	Andesite	Andesite	Basaltic andesite	Basaltic andesite	Andesite	Andesite
SiO ₂	61.85	65.74	52.0 ^a	65.70	61.26	65.06	59.51	59.39	56.35	54.03	60.29	58.36
TiO ₂	0.884	0.638	0.690	0.722	0.804	0.827	0.874	0.977	0.755	0.778	0.843	0.878
Al ₂ O ₃	15.55	15.25	19.40	14.31	15.67	15.00	17.14	15.84	18.89	19.41	16.10	16.13
Fe ₂ O ₃ *	8.99	5.79	9.97	7.47	8.36	7.52	8.16	9.41	7.90	8.69	8.57	9.04
MnO	0.224	0.187	0.175	0.187	0.208	0.191	0.210	0.226	0.170	0.179	0.203	0.224
MgO	1.97	1.03	4.36	1.45	1.82	1.17	1.94	2.36	2.12	2.56	2.33	2.39
CaO	5.50	3.86	10.26	4.50	5.44	4.22	5.56	6.15	8.17	9.08	6.04	6.22
Na ₂ O	4.12	4.74	2.46	3.90	3.99	4.27	4.02	3.93	3.60	3.44	3.73	4.41
K ₂ O	1.46	2.02	0.580	1.44	1.52	2.05	1.49	1.39	1.26	1.00	1.37	1.36
P ₂ O ₅	0.314	0.212	0.090	0.328	0.322	0.300	0.314	0.267	0.220	0.187	0.317	0.254
Total	100.9	99.5	100.0	100.0	99.4	100.6	99.2	99.9	99.4	99.3	99.8	99.3
LOI	0.76	0.55	nd	1.58	1.26	−0.06	1.62	0.15	0.46	1.70	2.39	3.09
Li	12.7	16.0	5.87	12.2	12.0	13.8	11.6	8.8	8.6	7.8	12.4	8.1
Be	1.03	1.23	0.408	1.07	1.06	1.27	0.991	0.819	0.770	0.661	0.892	0.816
Sc	26.5	19.8	31.8	21.6	23.4	20.5	23.1	23.0	22.1	25.7	24.7	26.3
V	98.1	26.1	266	53.2	79.5	22.6	68.9	144	141	188	108	142
Cr	4	4	14	0	1	5	1	1	0	1	3	1
Co	18.6	10.8	33.5	14.2	15.8	11.6	13.7	18.6	17.2	21.2	14.9	22.4
Ni	2.87	2.98	19.09	3.99	5.25	2.33	0.56	2.51	1.45	2.74	0.86	2.98
Cu	37	21	95	30	39	25	33	65	63	63	40	66
Zn	115	104	78.2	106	107	108	102	85	83	83	104	96
Ga	nd	nd	nd	nd	nd	nd	20	20	19	19	19	19
Rb	29.4	38.7	9.70	30.6	30.5	42.6	28.7	24.0	23.5	20.3	28.3	23.6
Sr	358	288	377	319	340	302	342	431	417	428	345	366
Y	40.9	47.0	19.6	42.1	41.6	47.0	39.1	30.5	29.7	27.3	35.0	33.3
Zr	123	159	49.4	130	126	171	118	95	91	79	106	98
Nb	2.89	3.48	0.94	2.95	2.88	3.64	2.94	2.34	2.23	2.59	2.54	2.48
Cs	0.773	0.988	0.290	0.777	0.762	0.936	0.720	0.611	0.595	0.528	0.681	0.585
Ba	425	524	190	444	435	538	405	342	331	280	374	357
La	13.2	16.0	4.39	13.9	13.7	15.9	12.6	10.2	9.8	8.2	11.3	10.8
Ce	28.0	33.5	9.75	29.4	29.1	33.7	27.7	22.2	21.4	17.9	24.8	24.0
Pr	4.12	4.88	1.50	4.34	4.28	4.92	4.27	3.41	3.13	2.72	3.65	3.70
Nd	19.3	22.4	7.39	20.2	19.9	22.6	18.8	14.9	14.4	12.3	16.8	16.8
Sm	5.29	6.04	2.22	5.46	5.46	6.08	5.10	4.00	3.90	3.41	4.56	4.59
Eu	1.69	1.73	0.84	1.68	1.68	1.76	1.58	1.30	1.27	1.15	1.43	1.44
Gd	6.54	7.25	2.91	6.71	6.57	7.32	6.02	4.74	4.57	4.05	5.37	5.24
Tb	1.09	1.24	0.51	1.13	1.11	1.24	1.01	0.80	0.77	0.69	0.91	0.89
Dy	6.88	7.76	3.30	7.00	6.97	7.78	6.33	4.98	4.85	4.38	5.66	5.50
Ho	1.48	1.66	0.71	1.50	1.49	1.65	1.37	1.08	1.04	0.95	1.23	1.18
Er	4.23	4.85	2.04	4.32	4.26	4.76	3.87	3.04	2.95	2.70	3.46	3.38
Yb	4.15	4.85	2.00	4.22	4.16	4.77	3.86	3.05	2.93	2.69	3.48	3.44
Lu	0.660	0.783	0.325	0.688	0.679	0.758	0.608	0.480	0.460	0.419	0.547	0.538
Hf	3.34	4.29	1.39	3.52	3.41	4.51	3.32	2.68	2.57	2.24	2.99	2.80

Table 2 (continued)

Sample name	Collected in May						Collected in April					
	Anat1	Anat2	Anat3	Anat4-p	Anat4-s	Anat9	04-Anat-01	04-Anat-02	04-Anat-03	04-Anat-04	Anat-26-01	Anat-26-02
Location	EM	EM	EM	EM	EM	WB	SW	SW valley	W cliff 1	W cliff 2	SW	SW
Sample type	Bomb	Lava	Lava with phenos	Scoria (P)	Scoria (S)	Lava	Scoria	Bomb	Bomb	Scoria	Ash/lapilli	Ash/lapilli
Rock type	Andesite	Dacite	Basalt	Dacite	Andesite	Dacite	Andesite	Andesite	Basaltic andesite	Basaltic andesite	Andesite	Andesite
Ta	0.212	0.265	0.076	0.220	0.218	0.272	0.198	0.157	0.152	0.177	0.180	0.173
Pb	5.65	7.26	2.55	5.96	5.75	7.13	4.95	4.23	4.09	3.50	4.81	4.32
Th	1.94	2.48	0.576	2.04	2.02	2.67	1.84	1.51	1.44	1.23	1.69	1.53
U	0.766	1.01	0.262	0.830	0.793	1.11	0.725	0.615	0.590	0.506	0.681	0.634

Major elements were acquired by ICP-AES and trace elements by ICP-MS at Boston University. Sample type refers to macroscopic description. Total Fe reported as Fe_2O_3^* . LOI=loss on ignition; WB=samples collected near the West Beach sampling site (N16°21'42.9", E145°38'03.5"); EM=samples collected at the East Meadow (no location available); SW=samples collected from layers in a beach cliff on the southwest side of the island (N16°20'8.8", E145°39'30"); SW Valley=a valley near the same landing site (N16°20'11.2", E145°40'43"); W cliff=samples collected from a cliff at a second landing site to the NW; (1) N16°20'13.2", E145°39'44"; (2) N16°20'21.4", E145°38'25.6".

^a SiO_2 calculated by difference.

ces on the pumice and scoria fractions, in order to obtain an internally consistent dataset.

2.2. Major and trace elements

Sample preparation and analytical procedures for all major and trace element analyses for the MARGINS and Woodhead samples analyzed at Boston University follow the techniques described in detail by Kelley et al. (2003). Solutions were prepared for major element analysis using LiBO_2 fusions, and each resulting solution was diluted $\sim 4300\times$ the original sample weight. Ten major elements were measured in these solutions using the Jobin-Yvon 170C ICP-AES at BU. Sample powders were prepared for trace element analysis following HF- HNO_3 digestion in Teflon screw-top vials, and resulting solutions were diluted to $\sim 2000\times$ the original powder weight. Thirty-five trace elements were measured in these solutions using the VG PQ ExCell quadrupole ICP-MS at Boston University. For a few samples of limited size, we determined major elements on the ICP-ES using the acid digests prepared for the ICP-MS. In these solutions, silica is volatilized by the HF procedure, and so estimated values are reported in Table 1 based on sum deficit. A few samples analyzed on the ICP-ES using both types of solutions (acid digest and

flux fusion) demonstrate that the sum deficit method provides very accurate silica, within 0.3 wt.% of the actual value.

Raw ICP-MS and ICP-ES counts were blank-subtracted, corrected for drift using an external solution (analyzed every five samples), and corrected for the dilution weight. USGS standards BHVO-1, W-2, and DNC-1 were used as calibration standards. Reproducibility of replicate ICP-ES and ICP-MS analyses is generally $<3\%$ RSD for the BU laboratories (Kelley et al., 2003), and variations observed in nearly identical Anatahan samples (e.g., Anat8p and 8s) suggest even better precision in these runs ($<2\%$ relative).

Rock samples collected by the USGS (Table 3) were prepared following the standard USGS methods described in detail by Taggart et al. (1987) and Taggart (2002). Samples were ground in a ceramic plate pulverizer. For major elements, samples were fused with lithium tetraborate into a glass disc, which was then analyzed by wavelength-dispersive X-ray fluorescence spectrometry (WDXRF). For trace element analysis, rock powders were left untreated and analyzed by instrumental neutron activation (INAA). New ICP-MS trace element data for rock samples collected by J.D. Woodhead (Table 4) were analyzed at Boston University using techniques described in Kelley et al. (2003).

Table 3

Major and trace element analyses for pre-historic Anatahan samples collected and analyzed by the USGS

Sample name	LAN90-19	MM92-45	LAN90-6	LAN90-10B	LAN90-18	LAN90-3	LAN90-12	LAN90-15	LAN90-16	LAN90-21	LAN90-9
Description	NW flow	Flow at caldera base	Southern flow	Eastern scoria	NW double crater	Pumice	Caldera collapse breccia	SE flow	NE flow	NW flow	Eastern flow
Rock type	Basaltic andesite	Basaltic andesite	Andesite	Andesite	Andesite	Andesite	Andesite	Andesite	Dacite	Dacite	Dacite
SiO ₂	52.4	53	57.9	59.4	60.4	62.2	62.4	62.9	64.6	65.1	65.9
TiO ₂	0.71	0.67	0.79	0.77	0.91	0.81	0.79	0.85	0.86	0.84	0.71
Al ₂ O ₃	19.5	18.1	16.8	13.8	15.7	14.6	15.4	14.9	14.6	14.5	14.8
Fe ₂ O ₃ *	9.31	9.99	8.89	7.34	8.92	7.84	7.31	8.13	7.53	7.39	6.19
MnO	0.18	0.19	0.2	0.19	0.22	0.21	0.2	0.21	0.2	0.2	0.18
MgO	3.93	4.92	3.01	1.74	2.36	1.52	1.75	1.57	1.22	1.15	1.05
CaO	10.8	10.1	7.39	4.38	5.97	4.54	4.9	4.79	4.15	4.04	3.71
Na ₂ O	2.48	2.5	3.55	5.6	3.95	4.66	4.4	4.38	4.33	4.34	4.71
K ₂ O	0.65	0.74	1.25	1.6	1.42	1.65	1.52	1.61	2.05	2.1	2.07
P ₂ O ₅	0.15	0.14	0.26	0.32	0.32	0.36	0.29	0.35	0.31	0.31	0.25
Total	100.1	100.4	100.0	95.1	100.2	98.4	99.0	99.7	99.9	100.0	99.6
Sc	34.3	37.3	28.8	21.1	25.6	22.6	22.3	23.8	21.0	21.2	18.1
Cr	12	10	5	1	2	2	1	0	1	2	2
Co	28.1	35.3	21.8	11.1	16.2	11.8	11.9	12.6	10.0	9.70	7.29
Ni	21.5	20.8	9.96	9.63	0	7.67	0.217	16.5	0	4.47	15.2
Zn	76.5	97.5	101	90	95	113	98	105	95	102	102
Rb	10.0	14.3	25.6	29.5	26.5	31.7	26.4	30.2	40.3	42.3	39.2
Sr	420	351	437	341	412	333	358	320	295	305	296
Zr	61.7	58.5	100	147	135	149	116	124	179	184	175
Cs	0.254	0.308	0.578	0.762	0.676	0.802	0.679	0.622	1.03	1.02	0.965
Ba	173	224	345	459	377	488	460	470	521	545	548
La	5.70	6.26	11.7	14.4	13.1	15.5	12.8	15.1	17.1	17.7	18.0
Ce	11.9	14.4	27.3	31.1	27.4	32.8	28.3	32.7	36.3	37.4	38.2
Nd	9.45	9.66	16.1	21.8	19.0	23.1	18.6	24.4	25.4	25.6	23.6
Sm	2.92	2.86	4.71	6.34	5.39	6.42	5.36	6.33	7.09	7.37	6.51
Eu	0.964	0.931	1.42	1.69	1.61	1.76	1.61	1.77	1.80	1.81	1.79
Gd	3.66	3.68	5.58	7.05	6.28	7.22	6.36	7.42	8.23	8.57	7.72
Tb	0.564	0.573	0.830	1.07	1.02	1.12	0.973	1.17	1.29	1.29	1.13
Ho	0.824	0.845	1.22	1.66	1.38	1.65	1.47	1.69	1.84	1.85	1.75
Yb	2.18	2.32	3.48	4.64	4.03	4.76	4.33	4.79	5.18	5.29	5.16
Lu	0.332	0.345	0.508	0.670	0.604	0.707	0.641	0.688	0.747	0.774	0.764
Hf	1.43	1.62	2.59	3.42	2.97	3.57	3.19	3.57	4.43	4.53	4.42
Ta	0.078	0.087	0.162	0.216	0.166	0.216	0.197	0.213	0.259	0.263	0.269
Th	0.682	0.929	1.62	2.10	1.88	2.20	1.79	2.11	2.72	2.84	2.69
U	0.305	0.358	0.623	0.859	0.733	0.907	0.797	0.840	1.130	1.230	1.080

Sample descriptions and locations in Moore et al. (1991, 1993). Major element data acquired by XRF, and trace element data by INAA. Total Fe reported as Fe₂O₃*

2.3. Sr, Nd, and Pb isotopes

Isotopic compositions of Sr, Nd, Hf, and Pb are listed in Table 5. ⁸⁷Sr/⁸⁶Sr was determined using the Finnigan MAT 261 solid-source mass spectrometer at UTD. Reproducibility of ⁸⁷Sr/⁸⁶Sr is ±0.00004. During the course of this work, the UTD laboratory

obtained a mean ⁸⁷Sr/⁸⁶Sr=0.70803 ± 3 for several analyses of the E and A SrCO₃ standard; data reported here have been adjusted to correspond to a value of 0.70800 for the E and A standards. ¹⁴³Nd/¹⁴⁴Nd was also determined using the UTD Finnigan-MAT261 in the dynamic multicollector mode. A total range of ±0.00002 was observed for ¹⁴³Nd/¹⁴⁴Nd of 13

analyses of the La Jolla Nd standard (mean value = 0.511846 ± 0.000013 , 1 S.D.) during November 2003, and is taken as the external precision for the samples. Redissolution and analysis of Anat 5 (unleached) in October 2004 were accompanied by $^{143}\text{Nd}/^{144}\text{Nd} = 0.511867$ for two analyses of the La Jolla standard and 0.512641 ± 11 for BCR. Nd isotopic compositions reported in Table 5 are adjusted to correspond to value of 0.511865 for the La Jolla Nd standard, which makes them comparable to results from Woodhead (1989). Calculations of ϵ_{Nd} for samples are based on CHUR $^{143}\text{Nd}/^{144}\text{Nd} = 0.512638$. Pb was separated using the technique of Manton (1988) and isotope ratios were also determined at UTD using the MAT 261 in the static multicollector mode and corrected for fractionation using results for the NBS-981 standard analyzed under the same conditions. Total processing blanks for Sr, Nd, and Pb are <0.1 , <0.3 , and <0.3 ng, respectively.

Also reported are new MC-ICPMS data on Pb isotopic compositions of 17 Anatahan samples using the methods described in Woodhead (2002). Instrumental mass bias was corrected using a Tl internal standard as described therein.

2.4. Hf isotopes

MARGINS samples analyzed for Hf isotopes were dissolved following conventional open-beaker digestion techniques, using doubly distilled HF, HCl, and HNO_3 acids. Hf was separated using procedures modified from Münker et al. (2001). Hafnium isotopes were measured on the ThermoFinnigan Neptune MC-ICPMS at UCSC. Total process blanks for Hf were <60 pg, and reproducibility of $^{176}\text{Hf}/^{177}\text{Hf}$ is ± 0.000008 (~ 2 S.D.), based on replicate analyses of 100 ppb solutions of JMC 475 over five analytical sessions (mean $^{176}\text{Hf}/^{177}\text{Hf} = 0.282146$; $n = 13$). $^{176}\text{Hf}/^{177}\text{Hf}$ ratios are accurate to ≤ 0.000005 based on replicate analyses of BCR-2 (0.282868 ± 0.000005 ; $n = 4$) and BRR-1 (0.283361 ± 0.000005 ; $n = 1$). These ratios and results for all samples are normalized to JMC 475 = 0.282160.

2.5. O isotopes and groundmass major elements

Oxygen isotope analyses were made on eight tephtras, three lavas, and one volcanic bomb from the

MARGINS May 2003 sampling. Groundmass was separated from the lavas and bomb by disaggregating each sample in a steel percussion mortar, and hand-picking aphyric fragments under a binocular microscope. Ashes were washed in de-ionized water and hand-picked to recover large (2–5 mm) clasts for analysis. These clasts are of two types: a vesicular, melanocratic glass that we refer to as scoria, and a highly vesicular, leucocratic glass that we refer to as pumice. Scoria and pumice samples have similar major element chemistry and phenocryst assemblages. Scoria samples have a greater proportion of magnetite as a groundmass phase. All hand-picked samples were lightly crushed in an agate mortar and dry-sieved to separate a 425–520 μm size fraction. Grains for analysis were hand-selected using a binocular microscope, sonicated in ethanol, and oven-dried at 120 °C before analysis.

Oxygen isotope ratios were determined by laser fluorination at the California Institute of Technology using a method based on that of Sharp (1990) and Valley et al. (1995). 1–2.5 mg aliquots were reacted with BrF_5 while heating with a 50 W, 10.5 μm laser. Product O_2 was purified, converted to CO_2 by reaction with hot graphite, and analyzed on a Finnegan MAT 251 stable isotope ratio mass spectrometer.

Samples were analyzed over 4 days, with a total of 19 aliquots of garnet standard, UWG2 (Valley et al., 1995), which gave an average reproducibility of $\pm 0.066\text{‰}$, 1σ . Based on the standard analyses, all sample measurements were corrected by between 0.12‰ and 0.18‰. The major element compositions of all oxygen isotope groundmass samples were determined on a Jeol JXA-733 electron microprobe in the Division Analytical Facility at the California Institute of Technology using a 15 kV accelerating potential, 25 nA sample current, and a 25 mm diameter beam. Oxide values were calculated using the CITZAF calculation package (Armstrong, 1995).

3. Composition of the new eruptions

3.1. Major and trace elements

Major and trace element data for samples that erupted in May are referred to as “May 03 samples”

Table 4
Major, trace, and Pb isotope values for Woodhead samples

Sample name	AN-1	AN-2	AN-3	AN-4	AN-5	AN-6	AN-7	AN-8	AN-10	AN-11	AN-12A	AN-12B	AN-12C	AN-12D	AN-12E	AN-12F
Rock type	Basalt	Basalt andesite	Basalt	Dacite	Basalt andesite	Andesite	Basalt Andesite	Basalt	Dacite	Basalt andesite	Andesite	Dacite	Dacite	Andesite	Dacite	Andesite
SiO ₂	51.66	52.31	50.01	63.39	53.71	58.15	53.49	49.28	63.91	53.31	62.83	63.31	63.13	62.82	63.11	62.96
TiO ₂	0.73	0.71	0.75	0.75	0.79	0.93	0.79	0.68	0.75	0.78	0.84	0.82	0.84	0.83	0.83	0.84
Al ₂ O ₃	18.54	21.18	20.18	15.62	18.45	15.63	18.63	20.09	15.47	18.54	14.98	15.03	15.03	15.12	14.99	15.13
Fe ₂ O ₃ *	10.3	8.77	10.3	7.24	10.5	10.6	10.37	10.6	7.03	10.38	8.25	8.14	8.24	8.27	8.21	8.31
MnO	0.19	0.16	0.18	0.20	0.20	0.21	0.20	0.19	0.20	0.20	0.23	0.22	0.22	0.21	0.22	0.21
MgO	4.97	2.88	3.86	1.59	3.26	2.70	3.29	4.51	1.52	3.36	1.64	1.55	1.59	1.60	1.59	1.59
CaO	10.3	10.6	11.4	4.71	9.23	6.53	9.33	11.8	4.56	9.43	4.84	4.70	4.83	4.82	4.80	4.83
Na ₂ O	2.53	2.76	2.35	4.27	3.02	3.93	3.06	2.22	4.38	3.16	4.43	4.19	4.34	4.33	4.26	4.13
K ₂ O	0.57	0.51	0.42	1.91	0.71	1.09	0.68	0.46	1.88	0.69	1.66	1.71	1.71	1.67	1.67	1.66
P ₂ O ₅	0.13	0.12	0.11	0.30	0.16	0.23	0.16	0.11	0.30	0.16	0.31	0.33	0.31	0.32	0.32	0.32
Li	5.25	5.28	4.16	13.6	5.82	12.3	6.36	4.40	13.7	5.90	11.8	12.4	4.81	8.18	12.5	6.45
Be	0.473	0.446	0.361	1.11	0.561	1.04	0.511	0.373	1.07	0.519	0.969	1.09	0.744	1.04	1.03	1.06
Sc	31.7	25.5	28.1	22.6	31.1	23.2	30.3	32.3	20.5	29.7	23.9	23.6	31.7	23.1	24.1	23.7
V	275	210	290	57.1	260	55.9	255	305	44.4	246	54.4	50.9	182	56.5	56.5	57.6
Cr	18	4	6	1	2	0	2	4	0	2	0	1	1	0	0	0
Co	31.6	30.6	27.8	11.5	43.3	30.9	25.7	33.0	9.1	37.7	43.6	12.7	22.4	12.2	12.8	12.7
Ni	17.84	9.90	13.80	2.67	6.39	3.52	6.08	14.72	1.46	5.87	0.873	0.993	1.20	0.376	0.985	0.853
Cu	116	85.4	136	16.9	115	31.3	105	104	14.7	124	31.8	33.9	41.7	31.6	32.7	32.9
Zn	76.9	66.8	68.1	94.1	86.6	97.1	77.6	71.3	89.8	81.2	89.2	103	94.0	98.1	104	90.3
Ga	15	17	16	14	17	14	16	16	14	16	11.9	14.0	15.1	13.9	13.5	13.7
Rb	11.6	9.50	6.36	36.8	13.2	32.0	11.7	10.5	36.8	12.0	31.06	32.7	17.49	30.59	32.30	28.35
Sr	382	445	436	336	418	327	414	447	323	408	327	338	355	331	341	341
Y	20.6	20.6	16.5	43.4	24.5	43.0	24.7	16.1	43.1	23.6	43.9	46.2	36.3	44.2	46.0	45.6

Zr	51.8	50.1	33.7	140	58.6	131	61.7	35.3	141	55.6	131	139	91.9	133	136	131
Nb	1.23	1.14	0.763	3.38	1.28	3.13	1.20	0.838	3.37	1.20	3.13	3.27	2.10	3.17	3.21	3.20
Cs	0.279	0.241	0.111	0.806	0.210	0.734	0.182	0.211	0.807	0.145	0.793	0.829	0.249	0.634	0.818	0.270
Ba	199	191	136	481	247	443	241	148	479	237	446	468	330	444	460	463
La	5.69	5.25	3.66	15.2	5.98	13.8	5.79	4.89	15.1	5.78	14.1	14.6	9.21	14.0	14.5	14.4
Ce	12.3	11.5	8.35	32.9	13.4	30.6	13.4	10.4	32.6	12.9	30.5	32.2	20.3	30.3	31.6	31.3
Pr	1.88	1.83	1.35	4.78	2.15	4.50	2.04	1.65	4.79	2.09	4.58	4.72	3.18	4.57	4.69	4.63
Nd	8.78	8.60	6.51	21.6	9.85	20.5	9.67	7.30	21.3	9.46	20.7	21.5	15.1	20.7	21.4	21.2
Sm	2.52	2.49	1.97	5.78	2.93	5.62	2.89	2.07	5.64	2.81	5.65	5.79	4.31	5.61	5.79	5.76
Eu	0.870	0.901	0.750	1.66	1.01	1.65	0.992	0.769	1.60	0.966	1.70	1.74	1.39	1.69	1.74	1.73
Gd	3.11	3.10	2.47	6.75	3.70	6.66	3.61	2.51	6.62	3.50	6.81	6.99	5.49	6.86	6.97	6.91
Tb	0.542	0.541	0.436	1.15	0.636	1.13	0.634	0.430	1.13	0.616	1.169	1.20	0.947	1.159	1.185	1.181
Dy	3.42	3.38	2.76	7.07	4.04	6.96	3.97	2.64	6.87	3.86	7.08	7.31	5.81	7.02	7.21	7.19
Ho	0.739	0.724	0.601	1.52	0.881	1.51	0.860	0.570	1.49	0.829	1.54	1.56	1.26	1.51	1.55	1.54
Er	2.08	2.03	1.68	4.34	2.49	4.24	2.42	1.60	4.21	2.37	4.37	4.47	3.60	4.35	4.44	4.42
Yb	2.10	2.07	1.67	4.37	2.47	4.28	2.43	1.57	4.26	2.37	4.33	4.46	3.50	4.32	4.43	4.39
Lu	0.329	0.322	0.266	0.693	0.389	0.674	0.387	0.246	0.670	0.368	0.688	0.704	0.565	0.686	0.704	0.697
Hf	1.49	1.41	0.989	3.77	1.69	3.51	1.67	1.02	3.72	1.60	3.68	3.82	2.65	3.71	3.76	3.68
Ta	0.0896	WC	0.0602	0.225	WC	WC	0.114	0.0581	0.272	WC	WC	0.226	0.175	0.232	0.223	0.222
Pb	2.42	2.34	1.60	5.65	2.80	5.22	2.34	2.37	5.55	2.73	5.78	6.07	3.85	5.56	5.84	4.60
Th	0.864	0.658	0.419	2.25	0.835	2.03	0.798	0.624	2.22	0.802	2.11	2.17	1.30	2.08	2.16	2.09
U	0.311	0.259	0.181	0.936	0.349	0.818	0.347	0.229	0.916	0.333	0.848	0.865	0.567	0.840	0.864	0.831
²⁰⁶ Pb/ ²⁰⁴ Pb	18.779, 18.781 ^R	18.790	18.792	18.795	18.795	18.805	18.800	18.769, 18.770 ^R	18.797	18.801	18.796	18.795	18.795	18.789	18.792	18.795
²⁰⁷ Pb/ ²⁰⁴ Pb	15.564, 15.565 ^R	15.564	15.557	15.564	15.565	15.566	15.568	15.563, 15.562 ^R	15.566	15.569	15.564	15.565	15.563	15.559	15.559	15.564
²⁰⁸ Pb/ ²⁰⁴ Pb	38.419, 38.424 ^R	38.418	38.398	38.422	38.418	38.427	38.427	38.416, 38.414 ^R	38.428	38.430	38.421	38.425	38.420	38.407	38.408	38.423

Total Fe reported as Fe₂O₃*. For convenience, previously published major elements are reproduced here (Woodhead, 1987, 1989). Trace elements acquired by ICP-MS at Boston University. Pb isotopes acquired at the University of Melbourne. Instrumental mass bias was corrected using a Tl internal standard as described in Woodhead (2002). SRM 981 Pb isotope standards run concurrently provided values, which are within error of the double spike-corrected numbers quoted by Woodhead et al. (1995). Superscript "R" indicates repeat analyses. WC indicates samples for which Ta was contaminated due to powdering in tungsten carbide.

Table 5

Radiogenic isotope data for May 03 samples

Sample name	Anat10			Anat5		
	Unleached	Unleached ^R	Leached	Unleached	Unleached ^R	Leached
²⁰⁶ Pb/ ²⁰⁴ Pb ^a	18.802		18.810	18.808		18.803
²⁰⁷ Pb/ ²⁰⁴ Pb	15.561		15.571	15.565		15.564
²⁰⁸ Pb/ ²⁰⁴ Pb	38.404		38.435	38.416		38.411
⁸⁷ Sr/ ⁸⁶ Sr ^b	0.703475 ± 13		0.703449 ± 17	0.703412 ± 11		0.703452 ± 12
¹⁴³ Nd/ ¹⁴⁴ Nd	0.512953 ± 19	0.512977 ± 10	0.512989 ± 8	0.512967 ± 13	0.512978 ± 7	0.512980 ± 16
ϵ_{Nd}	6.1	6.6	6.8	6.4	6.6	6.6
¹⁷⁶ Hf/ ¹⁷⁷ Hf	0.283200			0.283204		
ϵ_{Hf}	15.1			15.3		

Sr, Nd, and Pb isotopes were determined by solid-source mass spectrometry at the University of Texas at Dallas. Hf isotopes were measured by MC-ICP-MS at the University of California, Santa Cruz. ϵ_{Nd} and ϵ_{Hf} calculated using ¹⁴³Nd/¹⁴⁴Nd CHUR=0.512638 and ¹⁷⁶Hf/¹⁷⁷Hf CHUR=0.282772. Superscript “R” indicates redissolution and analysis. Nd and Hf ratios and results are reported relative to values of 0.511868 for La Jolla Nd and 0.282160 for JMC 475, respectively. Leached samples were leached in 2.5 N HCl for 1 h.

^a Corrected for fractionation using NBS SRM-981 ²⁰⁶Pb/²⁰⁴Pb=16.937, ²⁰⁷Pb/²⁰⁴Pb=15.492, ²⁰⁸Pb/²⁰⁴Pb=36.722.

^b Normalized to NBS SRM-987 ⁸⁷Sr/⁸⁶Sr=0.710233, equivalent in UTD laboratory to E and A ⁸⁷Sr/⁸⁶Sr=0.70800.

and are summarized in Table 1. Data for prehistoric samples collected by the MARGINS team in May 2003 and April 2004 (collectively called “MARGINS samples”) are summarized in Table 2. The rest of the data are divided into “USGS” (Table 3) and “Other” or “Woodhead” for Anatahan, and “Marianas” for the other islands (Moore et al., 1991; Elliott et al., 1997; Woodhead et al., 2001; Table 4). These distinctions between the different prehistoric Anatahan samples

are largely to distinguish variations caused by different analytical methods from those caused by magmatic processes. We assess here geochemical variability at increasing scales: from individual samples (pumice vs. scoria fractions), to the 2003 eruption, to the island of Anatahan and the Marianas as a whole.

Five samples were subdivided into pumice and scoria fragments, based on color and buoyancy. The

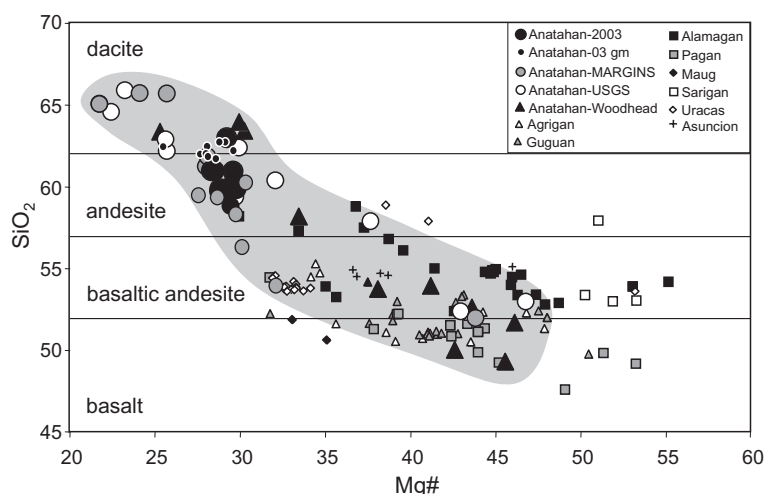


Fig. 3. Mg# (molar Mg/(Mg+Fe_T)) vs. silica content for volcanic rocks from the Mariana islands. Shaded region encloses full range of compositions at Anatahan. Data sources as follows: Anatahan—May 2003 and MARGINS samples from Tables 1 and 2. Anatahan—USGS from Table 3. Other Anatahan and Marianas data from Larson et al. (1975), Meijer (1976), Woodhead and Fraser (1985), Woodhead (1989), Woodhead et al. (2001), Elliott et al. (1997), and Table 4. Groundmass from May 03 tephra in Table 6.

geochemical data can be used to test whether these physical differences reflect different chemical compositions. Pallister et al. (2005—this issue) report no difference between pumice and scoria fractions, based on their XRF data. On the other hand, our ICP-ES data (Table 1) indicate a small, but consistent, shift in the major element compositions of the pumice vs. scoria samples. Pumice samples are consistently lower in mafic components, including MgO, Fe₂O₃, MnO, CaO, and TiO₂. Anat7 shows the largest range between pumice and scoria (~10%), but the differences in the other samples are generally small (within a few percent relative) and would not be detected with data of lesser precision, nor be as convincing with fewer pairs. These differences are consistent with the scoria samples having a higher proportion of mafic and oxide phenocrysts than the pumice sample. Such differences in phenocryst content would explain variations in those elements that are major constituents of the phenocrysts, but would have a lesser effect on trace elements, which do not show such consistent variation. A difference in phenocryst content is supported by backscattered electron imaging, which reveals an abundance of microphenocrysts of augite, plagioclase, and oxides in the dark “scoria” cores of lapilli, but few micro-lites in the outer “pumice” rims (Pallister et al., 2005—this issue).

There is very little variation within or between samples of the May 03 eruption. Silica contents vary from 59 to 63 wt.%, classifying most eruptives as andesites (medium K; Fig. 4), although some cross over into the dacite field (Fig. 3). The different samples within each lithotype (e.g., scoria, ash) differ by less than 3–4% on average, and there are few systematic variations throughout the stratigraphy shown in Fig. 2. The bottom fine ash (Anat5 and Anat11) has slightly lower Li and U concentrations (by 7–8%), and slightly higher Cu (by 11%) and Sr/Nd (by 5%) than the other May 03 samples. Aside from these subtle differences, there are no significant temporal variations in the first 10 days of the 2003 eruption of Anatahan (nor in the months that follow; Pallister et al., 2005—this issue). Taken together, all 12 samples fall within 3% (2σ) of the average 2003 composition for all 45 elements (excluding Ni and Cr, which are near the detection limit for the ICPMS data). The average of the bulk samples reported in de Moor et al. (2005—this issue) is within

3% relative to the major element average calculated here, and shows a similar lack of variation. Elemental ratios, such as Ba/La and U/Th (Fig. 5), vary less than 1.5% (2σ) about the mean of the 2003 samples. REE patterns for all 2003 samples are tightly clustered and parallel (Fig. 6). These variations in the May 03 Anatahan samples are largely a measure of our analytical precision.

The May 2003 eruption of Anatahan is compositionally very similar to eruptions in the past. Prehis-

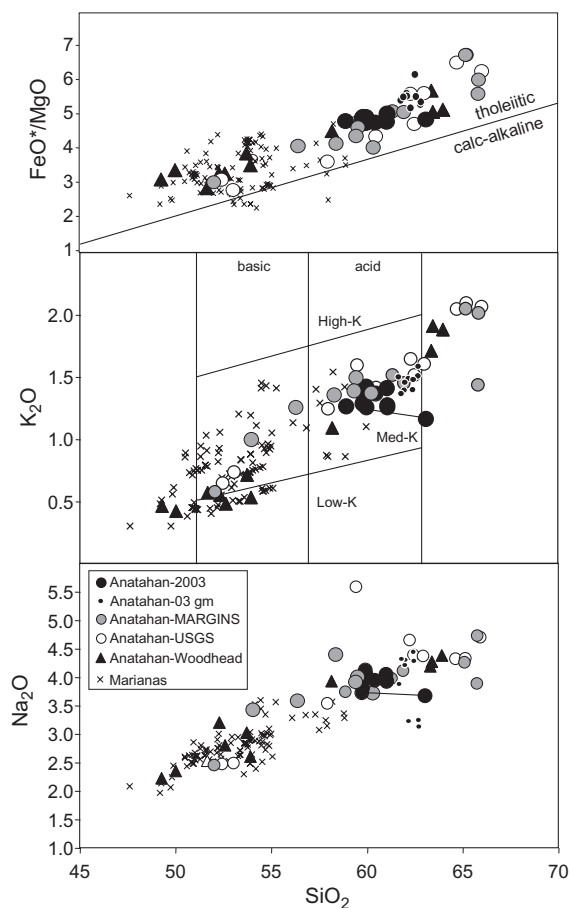


Fig. 4. Variation diagrams for Anatahan vs. other Marianas volcanics. Data sources as in Fig. 3. Tholeiitic/calc-alkaline boundary from Miyashiro (1974). K-divisions based on Gill (1981). Tie-line connects pumice (Anat7p) and scoria (Anat7s) pair. Anat7p plots to distinctly higher SiO₂ and lower K₂O and Na₂O than the rest of the May 03 samples. However, Anat7s plots squarely with the rest of the 2003 samples, and so these differences appear to be caused by pumice vs. scoria effects within sample Anat7, and not to a difference magma type. Data sources as in Fig. 3.

toric USGS samples LAN90-18, from the NW double crater, and LAN90-12, from a caldera collapse breccia deposit, are nearly identical to the average of the May 03 eruptives (within 7% and 9% on average for 45 elements, respectively). These variations could be mostly due to analytical errors or biases between the two laboratories (BU and USGS). This comparison demonstrates that Anatahan is capable of generating magma of nearly identical composition over time.

The homogeneity of the May 2003 eruption and the similarity to past eruptions may be a reflection of the similar parentage for most Anatahan magmas. On variation diagrams such as SiO_2 vs. K_2O (Fig. 4), almost all Anatahan volcanics lie on a single trend.

Incompatible trace element ratios are remarkably constant. For example, despite a factor of 4 variation in concentration, U/Th in Anatahan volcanics analyzed at BU varies by only 21% (0.455–0.360; Tables 1, 2, and 4 data only; Fig. 5). All the samples analyzed at BU have Ba/La of 30–37, except for four basalt/basaltic andesites (Ba/La=41–43; Anat3). The average Ba/La of the six most mafic samples (37 ± 5 , 2σ) is nearly the same as that for the six most felsic samples (32 ± 1 , 2σ). Variations in REE patterns are also systematic, with no crossing patterns, or unexpected variations (Fig. 6). As magmas evolve to more felsic compositions, REE concentrations, LREE/HREE, and the Eu anomaly increase.

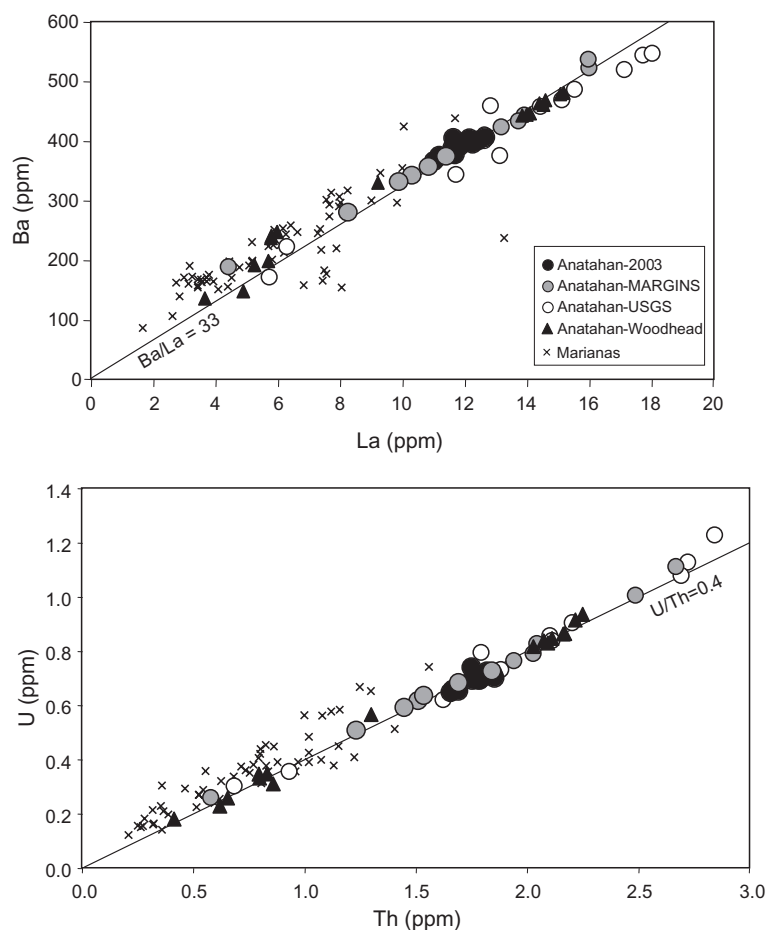


Fig. 5. Trace element variation in Anatahan vs. other Mariana islands. Lines of constant Ba/La and U/Th shown. The average Ba/La for the recent Anatahan eruptives is 33.2 ± 0.4 2σ , and the average U/Th is 0.395 ± 0.006 2σ ($n=12$). Both Ba/La and U/Th are lower in Anatahan volcanics than for most of the Mariana islands. Data sources as in Fig. 3.

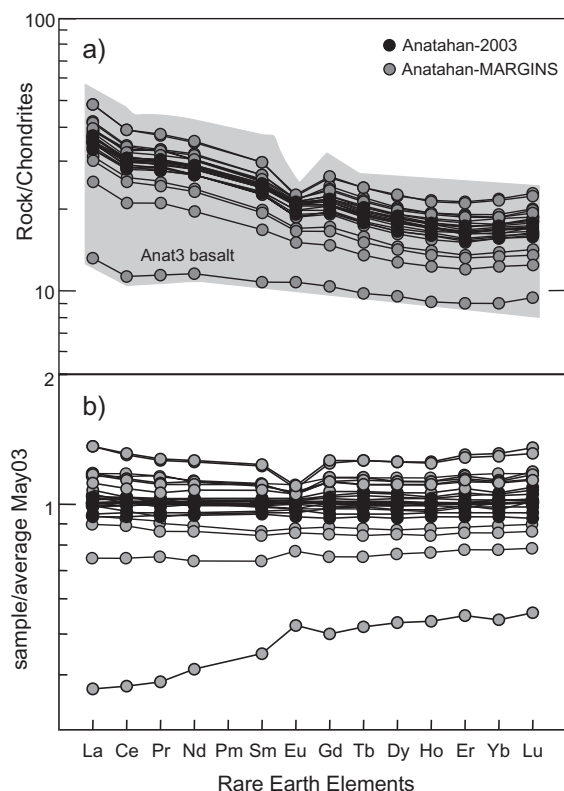


Fig. 6. (a) Chondrite-normalized rare earth element (REE) patterns of Anatahan volcanics (Nakamura, 1974). All patterns have the negative Ce anomaly characteristic of the Marianas arc (Dixon and Batiza, 1979; Hole et al., 1984; Elliott et al., 1997). The shaded field represents the full range of compositions at Anatahan. The basalt (Anat3) is depleted in REE relative to all other samples. (b) Samples normalized to the average May 03 eruptive. Only data from Tables 1 and 2 have been plotted, in order to avoid inter-laboratory biases.

Compared to the other volcanoes of the Mariana Islands, Anatahan is clearly unique. The other Marianas volcanoes erupt predominantly basalts and basaltic andesites, within a narrow range of SiO_2 from 50 to 55 wt.% (Fig. 3). Only Uracas, Alamagan (Moore and Trusdell, 1993) and Sarigan erupt andesites (>57 wt.% SiO_2), and andesites are common only on Anatahan (including the 2003 eruption). The only dacites in the active Mariana arc are found on Anatahan (although dacites and rhyolites have erupted in the past, as preserved in the 40 Ma submarine tephra record; Lee et al., 1995; Bryant et al., 1999). Aside from the predominance of evolved magmas, Anatahan otherwise has primary

characteristics that fall within the range of the rest of the Mariana islands. The mafic volcanics on Anatahan (<53 wt.% SiO_2) straddle the low–medium K_2O boundary (Fig. 4), similar to Guguan and Maug. Like most of the Marianas, Anatahan volcanics lie within the tholeiitic field (Fig. 4), and like most arc suites (Grove et al., 2003), Anatahan follows a trend that parallels the tholeiitic/calc alkaline boundary. Ba/La and U/Th are systematically lower (Fig. 5) in Anatahan than in many of the other islands (e.g., Guguan and Pagan). We will discuss in more detail below (Section 5) the origin of these trace element features of Anatahan magmas.

3.2. Isotopic compositions

$^{87}\text{Sr}/^{86}\text{Sr}$ (0.703450 ± 2) and $^{206}\text{Pb}/^{204}\text{Pb}$ (18.806 ± 5) isotopic compositions of May 03 samples (Table 5) are within the range of previously measured samples from Anatahan (Woodhead and Fraser, 1985; Woodhead, 1989; Woodhead et al., 2001). The older generation Sr and Pb isotopic data reported in Woodhead and Fraser (1985) span a large range for Anatahan, and some of this variation is likely to be analytical. There have been particular improvements in correcting for mass bias in Pb isotopic measurements, and new MC-ICPMS data show vast improvements in the Marianas dataset (see comparison of old and new generation Marianas data in Woodhead, 2002). Comparison of the May 03 samples to the new MC-ICPMS Pb data shows excellent agreement (Tables 4 and 5). Neither the Pb nor Sr isotopic compositions of Anatahan samples show any significant variation with silica (Sr; Fig. 7), as has been observed at other island arcs, such as the Lesser Antilles, where such variations have been taken as evidence for crustal contamination (Davidson, 1987).

The new Hf isotope data (0.283202 ± 4) for May 03 samples are within error of the two previously published results for Anatahan (Woodhead et al., 2001), although the new Nd isotope data are $\sim 0.5\epsilon_{\text{Nd}}$ lower. The new data are plotted in Fig. 8a together with results from samples from the Central Mariana volcanic front (Woodhead et al., 2001). Individual Mariana arc-front volcanoes have distinct Nd–Hf isotopic compositions, and all lie above the Terrestrial array of Vervoort et al. (1999). Samples from

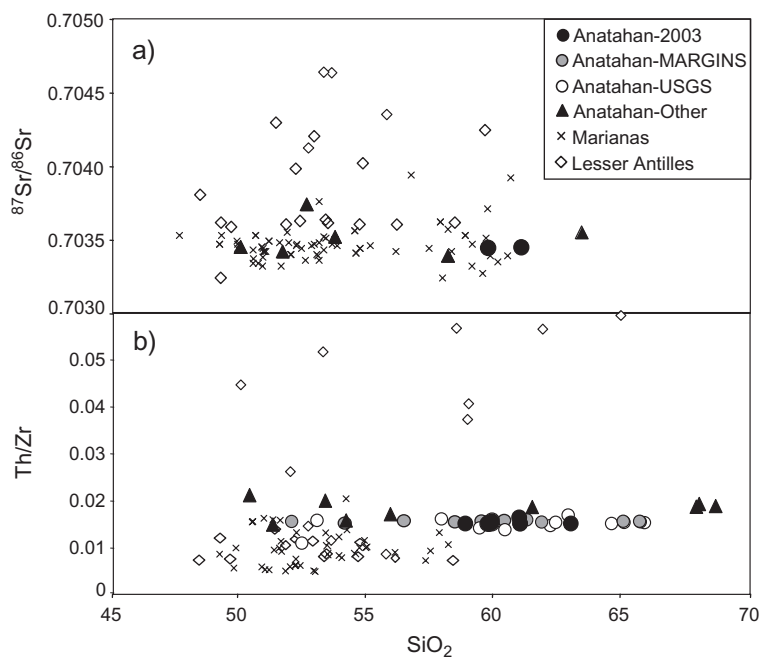


Fig. 7. Variation in (a) $^{87}\text{Sr}/^{86}\text{Sr}$ and (b) Th/Zr with SiO_2 for Anatahan, Marianas, and Lesser Antilles volcanics. The limited variation in $^{87}\text{Sr}/^{86}\text{Sr}$ and Th/Zr in the Marianas contrasts with that in the Lesser Antilles, which has been attributed to crustal contamination (Davidson, 1987). Several Lesser Antilles data points extend to $^{87}\text{Sr}/^{86}\text{Sr} > 0.709$ (omitted for clarity of Marianas data) and $\text{Th}/\text{Zr} > 0.3$. Marianas data sources as in Fig. 3, plus Table 5. Lesser Antilles data from Gravatt (1997) and Turner et al. (1996).

Guguan are the most radiogenic and samples from Anatahan and Sarigan the least. Anatahan has slightly higher ε_{Hf} at a given ε_{Nd} than Sarigan, but not outside of 2σ error. Hf trace element and isotope systematics are compared in Fig. 8b, in which Hf concentration anomalies (e.g., Hf/Hf^* ; for definition, see Fig. 8b caption) are plotted against ε_{Hf} for both published Mariana arc-front samples (data from Woodhead et al., 2001) and our new data for Anatahan (Tables 1 and 4). Hf/Hf^* ratios for May 03 Anatahan samples are similar to those calculated for the prehistoric Woodhead samples. Guguan and Alamagan samples have little or no Hf concentration anomaly; Agrigan samples have the largest anomaly; and Sarigan, Anatahan, Urcas, Pagan, and Maug are intermediate.

Oxygen isotope results are summarized in Table 6, and $\delta^{18}\text{O}$ values range from 5.5‰ to 6.1‰, with an average $\delta^{18}\text{O}$ of $5.70 \pm 0.3\%$ for all groundmass samples. The separated scoria and pumice fractions differ in measured $\delta^{18}\text{O}$. The dark-colored, less vesicular scoria fraction has an average $\delta^{18}\text{O}$ value

of $5.63 \pm 0.07\%$ ($n=8$), while the pumice fraction has an average $\delta^{18}\text{O}$ value of $5.86 \pm 0.08\%$ ($n=7$). The average fractionation between scoria and pumice samples is 0.26‰, and would be consistent with faster cooling and less degassing of pumice fragments than scoria fragments. Anatahan groundmass $\delta^{18}\text{O}$ values are similar to previously measured values for other Mariana arc lavas, which vary from 5.5‰ to 6.1‰, with an average value of $5.9 \pm 0.3\%$ (Eiler et al., 2000; Ito et al., 2003), and are typical for oceanic arcs as well as fresh MORB glasses (Eiler, 2001).

4. Magma evolution

Because Anatahan has erupted such a wide range of compositions, it provides an excellent opportunity to address questions of magma evolution in this classic island arc. The recent eruption of andesites with $>59\%$ SiO_2 at Anatahan is unique in the active Mariana islands, and reveals a different magmatic plumbing system for this volcano. The origin of high

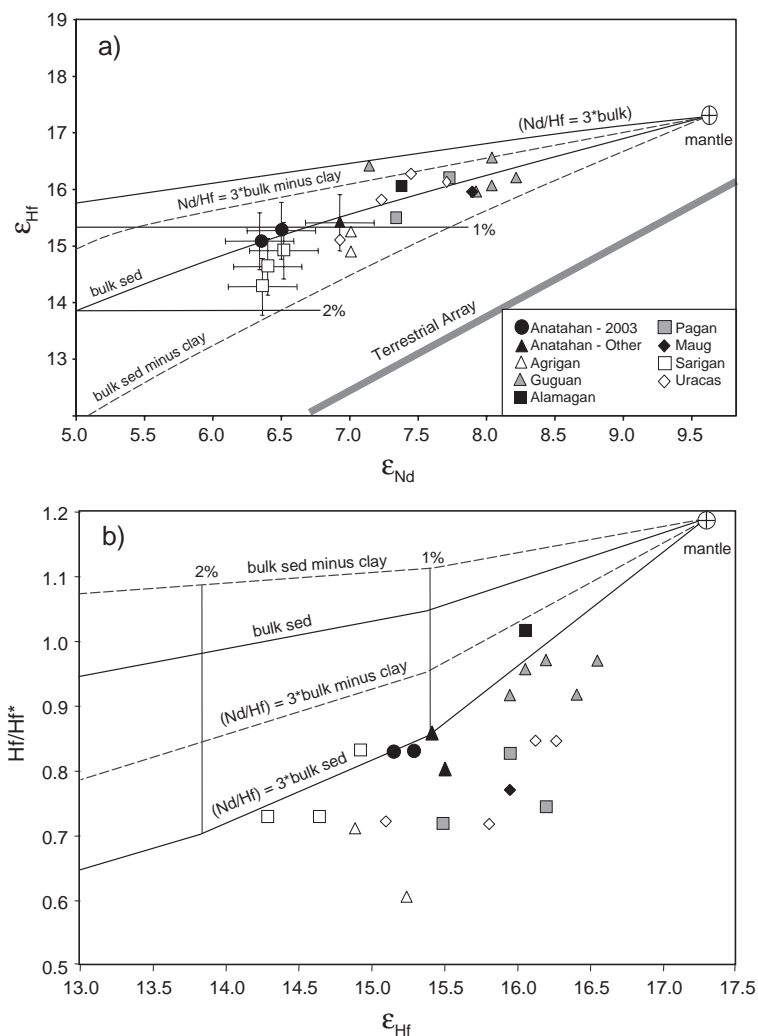


Fig. 8. (a) Nd–Hf isotopes for Anatahan lavas analyzed in this study (Table 5) and lavas of Marianas arc-front volcanoes (Woodhead et al., 2001). Also shown are two sets of mixing curves between Marianas mantle and subducting sediment (see Table 7 for end-member values used). Solid lines are for bulk sediment; dashed lines are for sediment with the top pelagic clay layer removed (using concentrations and mass fractions in Plank and Langmuir, 1998). Bulk sediment has $\epsilon_{\text{Nd}} = -2.24$, $\epsilon_{\text{Hf}} = +0.61$, and $\text{Nd}/\text{Hf} = 8.5$. Clay-free sediment has $\epsilon_{\text{Nd}} = -0.91$, $\epsilon_{\text{Hf}} = +0.24$, and $\text{Nd}/\text{Hf} = 6$. Other curves reflect an increase in the sediment Nd/Hf by a factor of 3 (to simulate the effect of zircon-saturated melting). Horizontal lines show constant percent sediment addition. Calculation of ϵ_{Nd} and ϵ_{Hf} uses $^{143}\text{Nd}/^{144}\text{Nd}_{\text{CHUR}(0)} = 0.512638$ and $^{176}\text{Hf}/^{177}\text{Hf}_{\text{CHUR}(0)} = 0.282772$, respectively. For 2003 samples, average unleached ϵ_{Nd} values are plotted. (b) Magnitude of Hf concentration anomaly (Hf/Hf^*) vs. ϵ_{Hf} for same samples and mixing curves as in (a). $\text{Hf}/\text{Hf}^* = \text{Hf}_n / [(\text{Nd}_n + \text{Sm}_n)/2]$, where the subscript “n” refers to trace element abundances normalized to chondritic values of McDonough and Sun (1995).

silica magmas (dacites and rhyolites) has long been debated by igneous petrologists, and is generally attributed to one of two origins: extensive crystal fractionation of mafic magmas or partial melting of crustal wallrocks. Once formed, high silica magmas can mix with mafic magmas to form intermediate

magmas, or be recycled by partial melting, but their initial formation requires either crystal fractionation of mantle-derived magmas, or partial melting of existing wallrock. Below we consider both of these end-member processes in the origin of Anatahan andesites and dacites.

Table 6
 $\delta^{18}\text{O}$ values and major element concentrations in Anatahan groundmass and plagioclase

Sample name Sample type	May 03 eruptives												Pre-historic eruptives							
	Anat5 g-p	Anat5 g-s	Anat6 g-p	Anat6 g-s	Anat7 g-p	Anat7 g-s	Anat8 g-p	Anat8 g-s	Anat10 g-s	Anat11 g-p	Anat11 g-s	Anat12 g-p	Anat12 g-s	Anat1 g-s	Anat2 g-s	Anat3 g-s	Anat3 plag	Anat4 g-p	Anat4 g-s	Anat9 g-s
$\delta^{18}\text{O}$	5.7	5.74	5.98	5.52	5.86	5.61	5.83	5.63	5.54	5.87	5.67	5.88	5.66	5.54	5.98	5.59	5.69	5.87	5.66	6.13
σ	0.07	0.12	–	0.14	0.04	–	–	–	–	0.05	0.06	0.11	0.00	0.04	0.13	0.02	0.06	0.26	0.10	0.00
SiO ₂	61.68			62.00	62.18	61.98	62.70	62.45	61.81	62.71			62.42							
TiO ₂	0.917			0.957	0.942	0.904	0.902	0.868	0.885	0.923			0.976							
Al ₂ O ₃	14.57			14.71	14.68	14.74	14.81	15.18	15.69	14.52			15.18							
Cr ₂ O ₃	0.00			0.00	0.00	0.01	0.01	0.01	0.01	0.01			0.01							
FeO*	8.28			8.28	8.15	8.43	8.30	8.08	7.39	8.39			8.05							
MnO	0.218			0.220	0.220	0.232	0.221	0.213	0.199	0.221			0.217							
MgO	1.86			1.81	1.92	1.81	1.91	1.77	1.62	1.90			1.54							
CaO	5.22			5.22	5.37	5.33	5.34	5.48	5.64	5.17			5.32							
Na ₂ O	3.89			4.31	3.23	4.22	3.26	4.30	4.33	3.14			4.45							
K ₂ O	1.51			1.46	1.50	1.40	1.52	1.49	1.37	1.59			1.40							
Total	98.15			98.98	98.20	99.05	98.96	99.84	98.94	98.57			99.57							

Groundmass samples (g) were separated into scoria (s) and pumice (p) fractions; “plag” indicates the plagioclase phenocryst analyzed. Isotope ratios were determined by laser fluorination at the California Institute of Technology. $\delta^{18}\text{O}$ analyses were corrected using the UWG2 standard to a value of 5.75‰, and corrections were 0.12–0.18‰. A total of 19 standards were run with an average $\delta^{18}\text{O}=5.87 \pm 0.7\text{‰}$. Major elements on the same groundmass separates determined by electron microprobe, also at Caltech. Note: These “p” and “s” fractions are from bulk samples independent of those described in Table 1. Total Fe reported as FeO*.

4.1. Crustal melting and assimilation

Here we consider a model whereby partial melting (anatexis) of pre-existing volcanic rocks generates rhyolitic magmas, which then mix with more mafic magmas to generate the andesites and dacites of Anatahan. Such a process is considered a form of crustal contamination, and is classically identified using isotope ratios (assuming isotopic contrasts exist within the crust). In continental arc settings, the isotopic composition of old crust will contrast greatly with that of mantle-derived magmas. Assimilation–fractional crystallization–mixing models that use old crust as a contaminant predict an increase in $^{87}\text{Sr}/^{86}\text{Sr}$, for example, as the magma evolves to more silicic compositions (Hildreth and Moorbath, 1988; Woodhead et al., 2001; Tamura et al., 2002). Such variations have been observed in volcanics from the Lesser Antilles island arc (Davidson, 1987), but are notably absent from the Marianas, including Anatahan (Fig. 7). For example, the $^{207}\text{Pb}/^{204}\text{Pb}$ isotopic composition of May 03 Anatahan andesites (15.561–15.565; Table 5) overlaps Anatahan basalts and basaltic andesites (15.557–15.569; Table 4). However, because old continental crust is absent from the Mariana arc, which is a young constructional feature (<50 Ma; Cosca et al., 1998), crustal melts will be little different isotopically from mantle melts. Nonetheless, there is a significant difference between the Hf–Nd isotopic composition of the modern Mariana arc (including Anatahan andesites and dacites; Table 5; Woodhead et al., 2001) and the 45–50 Ma Mariana protoarc (Pearce et al., 1999). This rules out direct derivation of Anatahan dacites as crustal melts of the protoarc. However, because of the small isotopic contrast between the protoarc and modern arc ($\sim 3 \epsilon_{\text{Hf}}$ units), it would be difficult to rule out other mixing scenarios.

Trace element ratios may provide another means of identifying crustal melting that is potentially more sensitive than isotopic systems in the Marianas arc. Silicic crustal melts should be in equilibrium with a mineral assemblage different from that of mafic melts, and accessory phase saturation, in particular, can be a useful test of crustal assimilation. As a magma evolves, Zr and P transition from incompatible elements when the magma is accessory mineral-undersaturated, to essential structural constituents

when the magma becomes saturated in zircon and apatite (Watson and Harrison, 1984; Evans and Hanson, 1993). As long as the magma remains zircon-undersaturated, Zr behaves as an incompatible element, and should co-vary with other highly incompatible elements (such as Th; see Fig. 9). The point of zircon saturation would be indicated by a kink in the fractionation trend, as the Zr concentration in the melt is then controlled by the solubility of zircon. This kind of behavior is observed in magmatic suites that evolve to rhyolitic compositions (e.g., Evans and Hanson, 1993 for the Batopilas region of Mexico), and for some submarine Izu rhyolites (Bryant et al., 2003). There are also many low Zr/Th rhyolites in the Mariana submarine tephra record, which could signal zircon saturation or a high-Th magma type (Bryant et al., 1999). The zircon solubility model of Watson and Harrison (1984) predicts that Marianas arc rhyolite would be zircon-saturated at 750 °C, if the melt has 100 ppm Zr (using a Miocene Marianas rhyolite composition in Lee et al., 1995 from DSDP53-1-1). Thus, if Anatahan magmas have mixed with such a melt, they should have variable Th/Zr. Instead, all Anatahan volcanics have the same Th/Zr, with no apparent change in the behavior of Zr (Figs. 7 and 9b). Anatahan dacites do not appear to have reached zircon saturation, nor is there evidence that they mixed with a zircon-saturated silicic crustal melt.

A similar kind of behavior to Zr can be expected for P, driven by apatite saturation (Fig. 9c). Here, Anatahan dacites do appear to reach apatite saturation (Fig. 9d). Phosphorous and Th increase together until magmas reach ~ 62 – 63 wt.% SiO_2 and 0.35 wt.% P_2O_5 , at which point P_2O_5 concentrations decrease, consistent with apatite saturation. Only sample Anat2 (a prehistoric dacitic lava) falls off the predicted trend, possibly reflecting mixing between an andesitic magma and a more evolved, apatite-saturated (but zircon-undersaturated) magma. The prediction of apatite saturation, but zircon undersaturation, of Anatahan dacites is consistent with solubility models. The apatite saturation thermometer in Piccoli and Candela (2002), which is based on the Watson and Harrison (1984) solubility model, predicts a temperature of ~ 970 °C for Anatahan dacites at the point of apatite saturation, which is very similar to the 1000 °C two-pyroxene temperature calculated for May 03

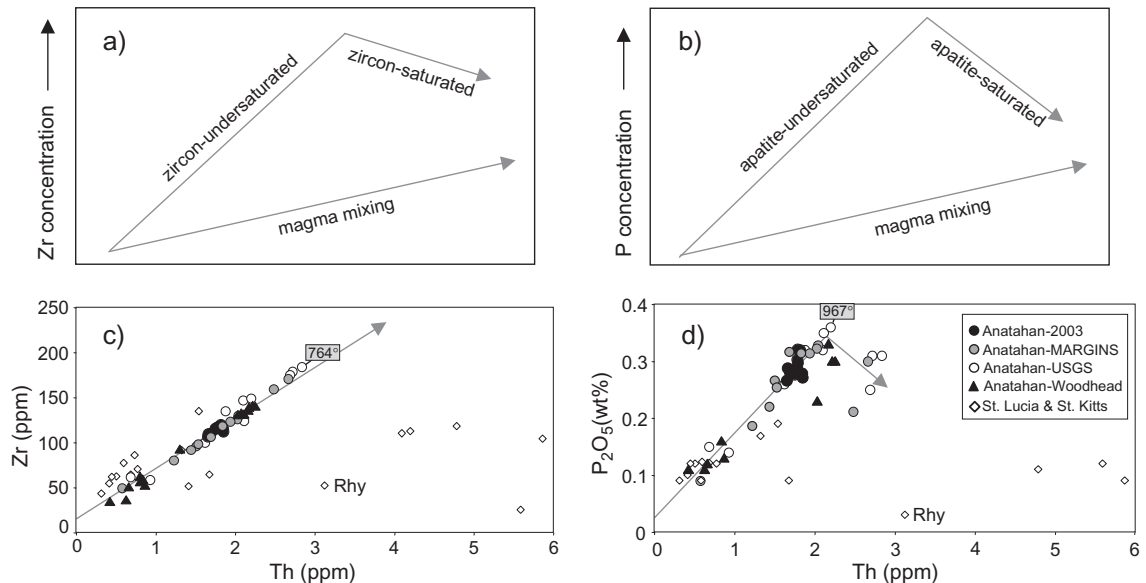


Fig. 9. Accessory mineral saturation in Anatahan magmas. (a and b) Schematic illustration of the evolution of two magmas, one which reaches phase saturation by crystal fractionation, and the other which mixes with a saturated magma (after Evans and Hanson, 1993). (c and d) Data for Anatahan and the Lesser Antilles volcanics. Anatahan volcanics indicate zircon undersaturation, and apatite saturation in dacites (at 0.35 wt.% P₂O₅). This is inconsistent with mixing with crustal melts, which are expected to be saturated in both apatite and zircon. Such mixing, or wholesale crustal assimilation, is indicated in the crustally contaminated Antilles volcanics. Data sources as in Fig. 7.

andesites (Pallister et al., 2005—this issue). On the other hand, dacites would be zircon-saturated only if the magma were at ~760 °C, an unreasonably low temperature for a dacitic liquid. Thus, the behavior of Anatahan magmas is consistent with predicted accessory mineral saturation models. If Anatahan dacites and andesites were generated by mixing with low-T rhyolitic crustal melts, then both P and Zr would reflect accessory mineral saturation. This behavior is observed in the Lesser Antilles, where several compositions appear to be mixing toward apatite- and zircon-saturated crustal melts (Fig. 9). Thus, this analysis suggests that while some island-arc volcanoes evolve through assimilation of crust (e.g., St. Lucia in the Lesser Antilles), Anatahan magmas did not.

Oxygen isotopes provide an additional constraint on crustal assimilation. The oxygen isotope compositions we observe for materials recovered from Anatahan could reflect, to greater or lesser degrees, any combination of effects from crystal fractionation, degassing, contamination by rocks in the upper plate through which they erupted, and/or addition to their mantle sources of components from the subducted

plate. In the following discussion, we first assess the relatively predictable effects of crystal fractionation and degassing, and then discuss the possibilities of crustal contamination.

Oxygen isotope fractionation between silicate melts and common silicate phenocryst phases is small (less than 1‰) at magmatic temperatures, but can drive measurable changes in the $\delta^{18}\text{O}$ values of magmas residual to high extents of crystallization (Taylor and Sheppard, 1986). We calculate the changes in $\delta^{18}\text{O}$ due to crystal fractionation likely undergone by magmas parental to Anatahan lavas and ashes using starting $\delta^{18}\text{O}$ values that span the range found in NMORB glasses (Eiler, 2001). This fractionation path predicts higher $\delta^{18}\text{O}$ by 0.1–0.5‰, than is observed in the Anatahan andesites (Fig. 10).

One possibility is that pre-existing, low $\delta^{18}\text{O}$ hydrothermal material contaminated the magma. Evidence for this lies in the active hydrothermal system present in the crater prior to eruption, and the orange grains of hydrothermally altered andesite ejected with juvenile andesite during deposition of the basal scoria unit (Pallister et al., 2005—this issue). If 7% of material with $\delta^{18}\text{O}$ of 0‰ is added to the

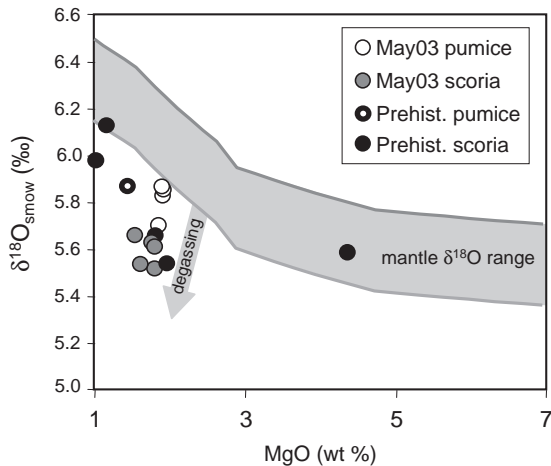


Fig. 10. MgO and $\delta^{18}\text{O}$ in groundmass samples from the May 03 eruption compared to calculated $\delta^{18}\text{O}$ variation during crystal fractionation. The fractionation trend was calculated using a Rayleigh fractionation model similar to those presented by Eiler (2001) and Cooper et al. (2004). Phase proportions predicted by pMELTS (Ghiorso et al., 2002) along the liquid line of descent for the Anatahan magma, and experimental and empirically estimated mineral-melt fractionation factors (summarized in Eiler, 2001) were used to calculate the equilibrium oxygen distribution between all phases at each 10° temperature step. Initial $\delta^{18}\text{O}$ is the full range of MORB (Eiler, 2001). The shift to lower $\delta^{18}\text{O}$ in the 2003 scoria vs. pumice may be due to degassing. The low $\delta^{18}\text{O}$ in Anatahan relative to the calculated fractionation paths, as well as the overlap between Anatahan andesites and MORB, argue against the evolution of Anatahan via crustal contamination. Data from Table 6.

magma, the $\delta^{18}\text{O}$ of the magma would be lowered by 0.5‰. Although possible, we find this an unlikely explanation for the samples analyzed here, which appear to have been deposited above the basal scoria, and do not contain such altered material.

Instead, we favor the degassing explanation outlined above as one mechanism for lowering $\delta^{18}\text{O}$ in Anatahan lapilli. The oxygen isotope difference between scoria and pumice recovered from Anatahan ashes is accompanied by a difference in vesicularity (the lower- $\delta^{18}\text{O}$ scoria is less vesicular than the higher- $\delta^{18}\text{O}$ pumice), with no significant difference in major element composition (Table 6). Although difficult to rule out, we find it unlikely that the difference in $\delta^{18}\text{O}$ is due to differences in the amount or source of crustal contaminants simply because the samples are compositionally similar to materials ejected from the same magma chamber during the same eruption. We suggest that their differences in $\delta^{18}\text{O}$ are generated

by differences in their degassing histories, where pumice fragments experienced less open system degassing of volatiles than did scoria samples. As a result, scoria underwent subtle (several tenths of per mil) ^{18}O depletion just before eruption by Rayleigh distillation loss of high- $\delta^{18}\text{O}$ volatiles, whereas the pumice did not (or did so to a lesser degree). To the best of our knowledge, this is the first suggestion that subtle oxygen isotope variations in volcanic glasses are generated by magmatic degassing processes. This scenario would predict that the pumice samples better record magmatic $\delta^{18}\text{O}$ and that the mismatch with the crystal fractionation model could be due to a later appearance of magnetite than that predicted by pMELTS (Fig. 10).

In summary, while we cannot exclude the possibility of some small (<7%) contamination of the 2003 Anatahan magma by pre-existing hydrothermally altered material, it appears to be inconsistent with the lack of variation in any of the chemical parameters except $\delta^{18}\text{O}$. On the other hand, the small shifts between observed and modeled $\delta^{18}\text{O}$ (<0.5‰) could be caused by degassing effects (which are consistent with observed vesicle contents) combined with uncertainties in the modeled proportions of phases that produce the kink observed in the calculated LLD.

Thus, four independent geochemical tests fail to uncover evidence for assimilation of felsic crust or crustal melts in the evolution of Anatahan magmas: (1) the lack of isotopic variation with silica in Anatahan magmas; (2) the lack of similarity between Anatahan dacites and Mariana protoarc basement; (3) the lack of zircon saturation recorded in trace element composition of Anatahan magmas; and (4) the MORB-like O isotopes of May 03 andesites. We also note that Pallister et al. (2005—this issue) found no evidence for mixing in the phenocryst populations from the recent eruptives, which are remarkably homogeneous, and in Mg# equilibrium with whole rock compositions. We also find it significant that U-series disequilibria provide further evidence against significant crustal derivation. Anatahan andesites have U–Th–Ra systematics similar to those of more mafic lavas from other Mariana islands. This is hard to reconcile with derivation of the andesites from cumulates that are even several millennia old. Instead, Reagan et al. (2005—this issue) argue that the

differentiation from basalt to andesite could have occurred within a few years in a closed system.

These tests do not completely rule out crustal melting in the origin of Anatahan magmas. It could be possible to produce Anatahan dacitic melts by direct partial melting of recent basalts with mantle $\delta^{18}\text{O}$, at high enough degrees of melting to exhaust zircon. Such a process, basically equilibrium melting of basalt, is of course very difficult to resolve from crystallization of basaltic liquid. However, if melting occurred fractionally, the first melts, formed at low temperature with high silica content, should be zircon-saturated. Such melts are not observed. Thus, to the extent to which we have the tools to resolve fractional melting from fractional crystallization, we favor fractional crystallization as the mechanism by which Anatahan magmas have evolved from basalt to dacite.

4.2. Quantifying crystal fractionation

The lack of evidence for crustal assimilation, the constant trace element ratios such as Ba/La, and the systematic REE patterns for Anatahan samples are all consistent with evolution by crystal fractionation of a common parental magma. Trace elements can be used to quantify the extent of fractional crystallization required to create the May 03 Anatahan magma from a parental basalt.

Enrichment factors are calculated by dividing the average of the May 03 eruptives by Anat3, the highest Mg# sample measured in the same laboratory. Fig. 11a compares these enrichment factors for a large suite of trace and minor elements. The enrichment factors should be related to the partition coefficients for the different elements, and so can be used as a measure of compatibility in the bulk solid fractionating phases. P, Th, and Nb show the maximum enrichment, being more than a factor of 3 higher in the May 03 eruptives than in the Anatahan basalt, and so are the most incompatible elements in the Anatahan magma series. Other elements show expected behavior, such as Zr and Hf having similar compatibility to each other, as well as to Nd and Sm (Pearce et al., 1999; Chauvel and Blichert-Toft, 2001). Ta is more compatible than Nb, which is consistent with cpx partitioning (Lundstrom et al., 1998). Other elements are notably

more compatible than inferred during mantle melting. For example, U is more compatible than Nb, and Cs and Ba are more compatible than Rb, and Pb is more compatible than Ce in Anatahan magmas; these element groupings are normally assumed to have identical partition coefficients to one another during mantle melting (Hofmann et al., 1986), but may not during fractional crystallization. We can use the most incompatible trace element (Th) to estimate the total proportion of crystals fractionated to create the May 03 andesite from basalt. If we assume that the bulk partition coefficient for Th is zero, then its enrichment is simply related to $1/F$, where F is the melt fraction. This calculation predicts 67% crystallization of the Anatahan basalt to produce the May 03 andesite, and 79% crystallization to produce the most evolved dacite (LAN90-9; Table 5).

The systematic REE patterns of Anatahan lavas invite us to estimate bulk partition coefficients during fractional crystallization. A bulk partition coefficient (D) can be calculated for each of the REE, using the fractional crystallization equation [$C_L/C_o = F^{(D-1)}$], with F as calculated above from Th, C_L from the average concentration of the May 03 magma, and C_o from the Anat3 basalt. Fig. 11b shows the resulting estimate of D for each REE. As expected, the LREE have lower D s (<0.3), and so are more incompatible than the HREE ($D=0.4-0.5$). The anomalously high D for Eu reflects the preferential partitioning of Eu^{2+} in the plagioclase structure. Given the observed and expected phenocrysts in Anatahan basalts and andesites (olivine, augite, low-Ca pyroxene, plagioclase, and Fe–Ti oxide; Pallister et al., 2005—this issue; de Moor et al., 2005—this issue), the mineral with the dominant control on the bulk D_{REE} will be augite (other D s will be much lower). Thus, the D pattern shown in Fig. 11b should mimic that for clinopyroxene if the May 03 andesite is related to the Anat3 basalt by crystal fractionation. In order to test this, we calculated the D_{REE} for an Anatahan clinopyroxene (Mg#=70; Pallister et al., 2005—this issue) using the model of Wood and Blundy (1997), at 1000 °C and 2 kb. This calculated cpx D pattern is very nearly parallel to the D pattern calculated for Anatahan. If cpx makes up 40% on average of the crystallizing assemblage (not unreasonable along

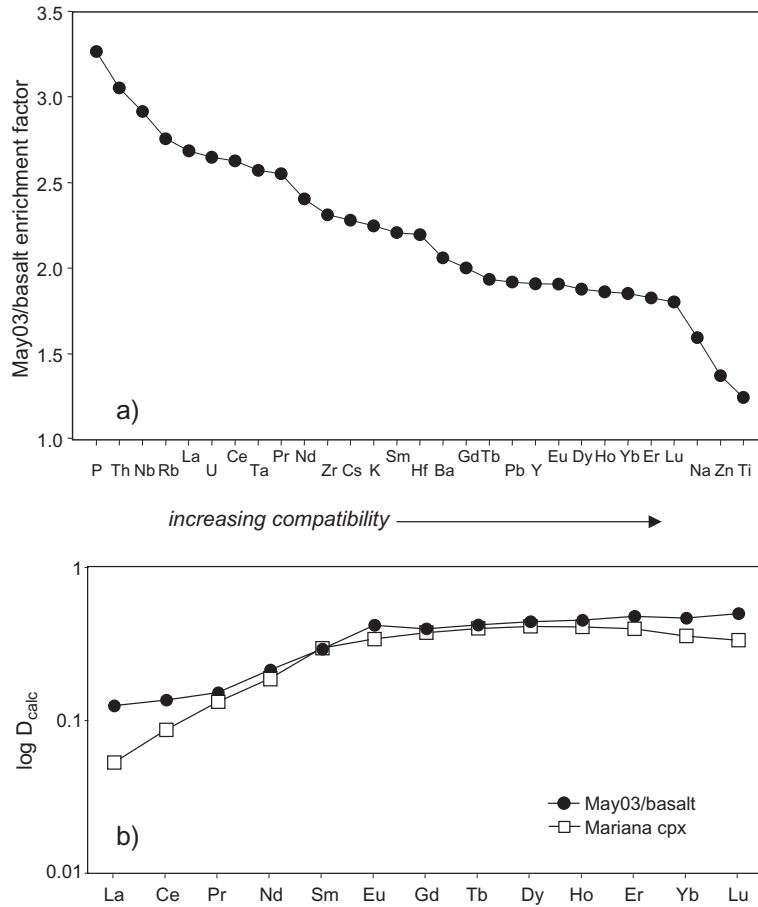


Fig. 11. (a) Enrichment factors calculated by dividing the average May 03 composition by Anat3, the most mafic sample measured in the same laboratory (a basalt/basaltic andesite). (b) Estimates of bulk partition coefficients for REE, calculated from enrichment factors in (a) and assuming fractional crystallization, compared to a model whereby cpx makes up 40% of the bulk crystallizing assemblage and has a D as predicted by Wood and Blundy (1997), and all of the other phases have $D=0$. See the text for a discussion of the model parameters.

the wet ol–plag–pyx cotectic, pMELTS; Ghiorso et al., 2002), then the predicted bulk D from cpx alone overlaps almost exactly that observed for Anatahan magmas. The discrepancies in the heaviest REE, and the lightest REE and Eu are presumably a consequence of assuming D of zero for the other phases (D_{Eu} and $D_{LREE} \gg 0$ in plag and $D_{HREE} \gg 0$ in opx). Clearly other combinations of temperature, pressure, and cpx mode will also produce satisfactory fits. The main point is that the dominant shape of the D pattern is successfully reproduced by the D for cpx, using reasonable input parameters for crystal fractionation of Anatahan magma.

5. Recycled material from the subduction zone

Subduction zone magmas are mixtures of mantle melt, which dominates the budget for major elements, and fluids from the subducting plate, which contribute trace elements to the sub-arc mantle (see reviews in Gill, 1981; Tatsumi and Eggins, 1995; Elliott, 2003; Kelemen et al., 2003). The Marianas region has been designated an NSF-MARGINS focus area, in part because of the excellent control on volcanic outputs and crustal inputs to the subduction zone. During ODP Legs 129 and 185, several holes were drilled in the seafloor seaward of the Marianas trench, providing unusually good sampling of subducting material. The

~450 m sedimentary section consists of ~50 m of pelagic clay at the top, underlain by ~50 m of chert, ~200 m of volcanoclastic turbidites, and ~150 m of radiolarite (Lancelot et al., 1990). The pelagic clay unit, although the thinnest, is the most enriched in many trace elements, and so its fate is of importance to the geochemical recycling problem (Plank and Langmuir, 1998). Being the top unit with the greatest porosity, the pelagic clay is also the most vulnerable to loss from the slab by shearing or underplating, and so of importance to the dynamics of sediment delivery to the sub-arc mantle. The volcanoclastic section derives from the numerous Cretaceous seamounts that litter the seafloor, including the Magellan and Wake seamount provinces (Abrams et al., 2001; Castillo et al., 1992). These seamounts are particularly heterogeneous in their isotopic compositions, spanning virtually all known oceanic island geochemical provinces, including HIMU, EMI, and EMII types (Koppers et al., 2003a). Their variable distribution on the seafloor can generate significant heterogeneity in the subducting input (Plank and Langmuir, 1998), and can have a large effect on the isotopic variability observed in the Marianas arc (Pearce et al., 1999). Beneath the sedimentary section is the oldest oceanic crust in the modern ocean (170 Ma; Bartolini and Larson, 2001; Koppers et al., 2003b), which was formed at intermediate-to-fast spreading rates at southern latitudes (Pockalny and Larson, 2003). Its primary composition is typical of modern Pacific MORB (Fisk and Kelley, 2002) and seawater alteration has affected its inventory of trace elements (Kelley, 2003).

Certain aspects of the isotopic and trace element composition of Marianas arc volcanics can be traced back to both the sedimentary and basaltic layers on the subducting Pacific Plate. The basaltic component contributes low $^{87}\text{Sr}/^{86}\text{Sr}$ and low $^{207}\text{Pb}/^{204}\text{Pb}$, like MORB, but high Pb/Ce, U/Th, and Ba/La relative to MORB (Elliott et al., 1997). These trace element fractionations are thought to originate from aqueous fluid partitioning, as altered oceanic crust dehydrates in the subduction zone (Elliott et al., 1997; Lin et al., 1990; Woodhead, 1989). The sedimentary component contributes REE (negative Ce anomalies, and low $^{143}\text{Nd}/^{144}\text{Nd}$), Nb anomalies, and high Th/La. These elements are not readily partitioned into sediment dehydration fluids (Johnson and Plank, 1999), and so are more likely mobilized out of the

slab via a sediment melt (Elliott et al., 1997; Hermann, 2002; Turner et al., 1996). These two components—a basaltic fluid and a sediment melt—mix in varying proportions to generate unique geochemical fingerprints for each of the Mariana islands. Guguan island records the greatest basalt fluid flux, and Agrigan island the greatest sediment flux. The new geochemical data on Anatahan volcanics presented here can be used to explore its unique record of recycled material from the subducting plate. Our goal here is not to argue for one model or another, but to quantify subducted contributions to Anatahan based on the basalt fluid, sediment-melt model argued by Elliott et al. (1997) for the Mariana arc as a whole.

5.1. Trace element ratios

The Mariana islands record a factor of 3 variation in Ba/La, from ~20 in Agrigan to up to 60 in Guguan (Fig. 12b). All of these values exceed normal MORB (Ba/La=2–5; see references in Fig. 12 caption), and altered oceanic crust (~5; Kelley et al., 2003), and many exceed estimates of the bulk subducting sediment (Ba/La=7–35; Plank and Langmuir, 1998). Instead, high Ba/La is ascribed to slab basalt fluid (e.g., Woodhead, 1989; Lin et al., 1990), in part because it is highest in those volcanics that have the highest $^{143}\text{Nd}/^{144}\text{Nd}$ (most MORB-like). Low Ba/La volcanics have the greatest negative Ce anomalies and LREE enrichment, characteristics attributed to derivation from the subducting sediment (Elliott et al., 1997). In fact, Ba/La correlates with LREE depletion (e.g., Sm/La; Fig. 12b), and the variation in the Marianas as a whole is well explained by mixing between a slab sediment melt (with low Ba/La and Sm/La) and a MORB mantle that is enriched in Ba from slab fluids (with high Ba/La and Sm/La). There is a significant amount of variation in the bulk sediments on the seafloor seaward of the trench (between sites 800 and 801), particularly in Ba/La, which is dependent on the proportion of pelagic clay (highest REE concentrations, so lowest Ba/La) to basal radiolarite (which may have high Ba from hydrothermal input). The dispersion of the Marianas array suggests greater variability in the sedimentary end-member, consistent with the variations on the seafloor and variable survival of the pelagic clay

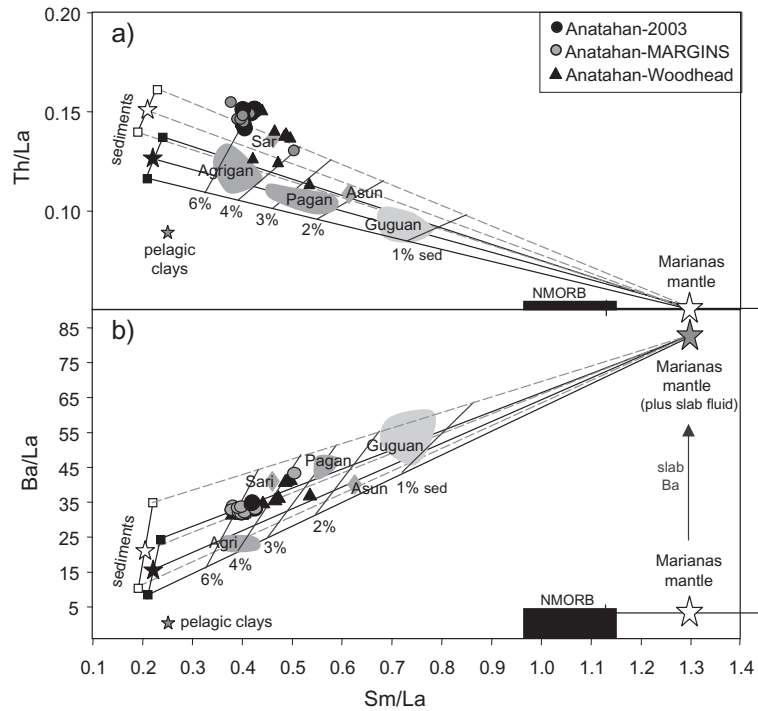


Fig. 12. Trace element ratios record mixing between mantle and subducted sediment in the source of Marianas magmas. Black and white stars represent the average Marianas bulk sediment, while flanking squares represent a range in sediment composition (estimates from ODP Sites 800 and 801; Plank and Langmuir, 1998). Filled sediment symbols represent bulk sediment, while open sediment symbols represent sediment after removal of the top pelagic clay unit (shown). 1–4 wt.% bulk sediment in the mantle source indicated as crossing lines. Anatahan data plotted were collected at BU (Tables 1, 2, and 4); other Marianas data from Elliott et al. (1997). (Note: Gug3 plots with Agrigan, and is removed from the figure for clarity). Only May03 or more mafic samples are plotted, in order to better evaluate the parental magma. Samples which were found to be apatite saturated (see Fig. 9) have also been removed. Sm/La mantle estimate with uncertainty from Plank (in press).

section, and less variation in the high Ba/La fluid end-member (Fig. 12b).

Anatahan falls at the low Sm/La end of the Marianas array. As discussed above, magma evolution leads to no significant change in Ba/La in Anatahan, although more felsic compositions will have lower Sm/La, due to the crystal fractionation effects discussed in Section 4.2. This will lead to some dispersion parallel to the X-axis, but does not change the position of Anatahan significantly relative to the other Mariana islands. Low Sm/La and Ba/La are consistent with a relatively high proportion of recycled subducted sediment in Anatahan sources, similar to Agrigan, Sari, and Uracas islands in this regard. Anatahan appears to mix to a sedimentary component with higher Ba/La than the average Marianas sediment, and more similar to Site 801 sediment, or sections where the

pelagic clay unit has removed from the subducting plate.

Th/La is another useful trace element ratio in constraining the mixing end-members of arc magma sources. Arcs worldwide have Th/La higher than MORB, and mix to sedimentary compositions in most cases identical to those outboard of the trench (Plank, in press). The Marianas is no exception. The arc as a whole forms a Th/La–Sm/La mixing array between local sediment, and a mantle similar to, but more LREE-depleted, than N-MORB (Fig. 12a). This projected mantle composition has the same Sm/La as that on the Ba/La diagram, and so these two systems provide a coherent estimate of the composition of the background mantle beneath the Marianas arc. Note that Th and REE, however, require no additional fluid component, and are wholly explained by mantle–sediment mixing. This

again provides evidence for a lack of partitioning of Th and REE in aqueous fluids, but mobilization in sediment melts. While most of the Mariana islands mix between the mantle and the average Marianas sediment value, Uracas, Alamagan, Sarigan, and especially Anatahan mix to a sediment with higher Th/La than the range represented by ODP 800–801 (Fig. 12a). Removal of the top pelagic clay unit, which is the most REE-enriched, shifts bulk values to higher Th/La. Thus, the sediment that subducts beneath Anatahan may have lost its upper pelagic section (~50 m) to underplating.

Mixing on both the Ba/La and Th/La diagrams is highly constrained by Sm/La, which varies by more than a factor of 6 between the mantle and sediment end-members. Mixing between mantle and bulk Marianas sediments predicts 1–6% sediment in the source of Marianas volcanoes, with the least for Guguan (1%) and the most for Agrigan (6%). Anatahan volcanics require 3–6% sediment, at the high end of the Mariana spectrum. The highest estimates are for Anatahan andesites, which have elevated Sm/La in part due to crystal fractionation (as discussed above). Consideration of just the Anatahan mafic magmas ($\leq 55\%$ SiO₂) leads to $4 \pm 1\%$ sediment. Because the mixing proportions are so highly dependent on Sm/La, it is possible to shift the results significantly by changing Sm/La in the sedimentary end-member. If the sediment is contributed as a melt, then it is highly likely that Sm and La will be fractionated from one another, with the melt preferring the LREE. The experiments of Johnson and Plank (1999) indicate a decrease in Sm/La by a factor of 1.6 (at 800 °C). Such a decrease would shift the 1–6% melting contours to 0.8–4%, and mafic Anatahan magmas to ~3% sediment, in better accord with the isotopic mixing results below.

5.2. Pb isotopes

The first evidence for subducted sediment in the source of arc volcanics came from Pb isotope mixing trends (Tatsumoto and Knight, 1969; Kay et al., 1978; Sun, 1980), but the interpretation of such trends has been controversial due to the overlap between arc and mantle compositions (Morris and Hart, 1983), the effects of crustal contamination (Kersting et al.,

1996), and the similarity between the slope of arc arrays and the slope of mass fractionation in Pb isotopic measurements, particularly for ²⁰⁷Pb/²⁰⁴Pb. The case for the Marianas has been obscured by overlap between much of the arc and normal MORB mantle (Meijer, 1976). However, in new-generation MC-ICPMS Pb isotope data (Woodhead, 2002), where mass fractionation errors have been dramatically minimized, the Marianas arc clearly forms a steep array in ²⁰⁶Pb/²⁰⁴Pb–²⁰⁷Pb/²⁰⁴Pb, which is consistent with mixing between Pacific MORB Pb and bulk sediment Pb (Fig. 13). The uniformly low Ce/Pb of Marianas volcanics (3–8) is analogous to their high Ba/La, and requires that the mantle end-member contain a large fraction of MORB fluid-derived Pb. Such a case was illustrated clearly for the Aleutians (Miller et al., 1994) and applies equally to the Marianas. The “mantle” Pb end-member on the isotope diagram (Fig. 13) cannot be mantle only; otherwise Marianas volcanics would mix to high Ce/Pb (>25), which they do not. Instead, 94% of the Pb in the “mantle” end-member appears to be Pb-derived from the subducting Pacific MORB (based on Ce/Pb of the mantle+fluid of 2, and depleted mantle values from above; Table 7). The sedimentary end-member is a composition similar to the bulk sediments at ODP Sites 801 and 800 (as given in Plank and Langmuir, 1998), although the very large range in pelagic and volcanoclastic end-members (which could span the entire range from HIMU compositions like the South Wake seamounts to the low ²⁰⁶Pb/²⁰⁴Pb compositions of the Magellan seamounts; Koppers et al., 2003a), combined with the paucity of sedimentary Pb isotopic measurements (none of which are “new generation”), leads to considerable uncertainty in the bulk sediment composition. Nonetheless, using the current sediment estimates, the sediment mixing proportions for the Marianas arc (1–4%) and Anatahan (2.5–3.5%) are very similar to those derived above independently for the trace elements. Removal of pelagic clay in this case has a small effect on the mixing relationships (Fig. 13) because sediments plot far from the arc field.

5.3. Hf and Nd isotopes

Nd–Hf isotopes of Mariana arc-front volcanoes are also generally consistent with the addition of Mariana sediment. Mixing of bulk sediment can account for

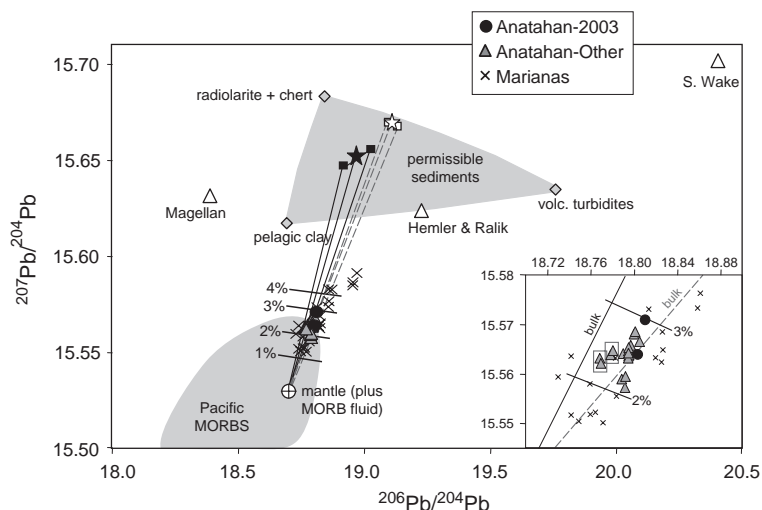


Fig. 13. Pb isotopes in Anatahan and other Mariana islands. Diamonds represent lithologic units from Plank and Langmuir (1998). Open triangles represent seamounts from Koppers et al. (2003a), which are the source of volcanoclastic sediments to the Marianas trench. Black and white stars and boxes represent Marianas bulk sediment (as for Fig. 12). 1–4 wt.% bulk sediment in the mantle source indicated as crossing lines (using end member values given in Table 7; see text). Inset shows Anatahan samples, with bulk mixing lines. Boxes enclose repeat analyses. Anatahan data from Tables 4 and 5; Marianas data are new MC-ICPMS data from J.D. Woodhead (unpublished).

the variations of Nd and Hf isotopes of Mariana volcanoes if the sediment contains a pelagic clay component, but the sediment component needs to have an elevated Nd/Hf ratio if the pelagic clay is removed (Fig. 8a). Preferential transport of sedimentary Nd relative to Hf would occur if sediment melts in the subducting plate are zircon-saturated, which would be expected given their silicic compositions (and was observed in the experiments of Johnson and Plank, 1999). Zircon strongly partitions Hf, and its presence has a large effect on Nd–Hf mixing calculations. Nd–Hf isotopes of Mariana arc-front volcanoes are consistent with the addition of 0.5–2% recently subducted sediment to the depleted mantle source (Fig. 8a). The most radiogenic Mariana arc-front volcanoes (e.g., Guguan) require < 1% sediment, whereas the least radiogenic (including Anatahan) require < 2% sediment.

The magnitude of Hf concentration anomalies (Hf/Hf*) is difficult to achieve with the same mixing models that satisfy the isotopes. All mixing curves lie above the Marianas data. This is partly due to using the depleted mantle of Salters and Stracke (2004), which has a positive Hf anomaly. Even with a mantle with no Hf anomaly, however, mixing lines still lie above most of the Mariana array. This indicates that

Table 7

Compositions used for mixing calculations

End member	Depleted mantle	DM with fluid	801 bulk seed
La	0.200	0.200	18.8
Ce	0.690	0.690	29.4
Nd	0.670	0.670	20.8
Sm	0.259	0.259	4.43
Hf	0.191	0.191	2.44
Th	0.010	0.010	2.58
Ba	1.0	16.0	442
Pb	0.021	0.345	6.60
$^{206}\text{Pb}/^{204}\text{Pb}$	–	18.70	18.92
$^{207}\text{Pb}/^{204}\text{Pb}$	–	15.53	15.65
$^{143}\text{Nd}/^{144}\text{Nd}$	0.51313	0.51313	0.51252
$^{176}\text{Hf}/^{177}\text{Hf}$	0.28326	0.28326	0.28279

Depleted mantle based on Salters and Stracke (2004). However, their composition is too low to serve as an adequate end-member, based on linear mixing relationships shown in Fig. 12. We use Sm/La=1.3 ± 0.35, which was calculated by Plank (in press) by regression through Marianas basalt data, and conforms to the data arrays in Fig. 12. The depleted mantle of Salters and Stracke (2004) was adjusted to this value of Sm/La by removing a small degree melt (0.13%) to arrive at these values. Nd and Hf isotopes from Woodhead et al. (2003) for the most radiogenic N. Mariana Trough basalt. Mantle with fluid assumes no REE nor Hf in fluid, and satisfies Ba/La=80 (from Fig. 12b) and Ce/Pb=2 (see text). Pb isotopes to satisfy mixing models in Fig. 13. ODP Site 801 bulk sediment from Plank and Langmuir (1998). Hf isotopes calculated using weighted means of lithologies, and isotopic data in Pearce et al. (1999) and Woodhead et al. (2001).

the bulk Marianas sediment does not have a sufficiently large Hf concentration anomaly to drive down the mixing lines, and only if Nd and Hf are fractionated by a factor of 3 (simulating the effect of zircon) do curves approach the data array, specifically the Anatahan andesites. These same calculations, however, fail to explain the isotopic data. Thus, bulk sediment mixing explains the isotopes, but not the concentration anomalies. Zircon-saturated sediment melts (high Nd/Hf) may explain concentration anomalies, but not the isotopes. Addition of clay-free sediment (for Th/La) requires even more fractionated Nd/Hf to compensate for the loss of Nd/Hf-rich clay. Nonetheless, we emphasize the few Hf isotopic measurements available ($n=6$), on widely varying lithologies (clay and volcanoclastics) to constrain sedimentary end-members. While no existing model explains quantitatively both Hf–Nd isotopes and concentrations, sediment addition works in a general sense to create correlated isotopic and Hf anomaly variations in Marianas lavas, in mixing proportions that agree in magnitude (e.g., a few percent) with results from Pb isotopes and trace elements. Further work characterizing the isotopic compositions of subducting sediments will help constrain this model.

5.4. Summary of mixing calculations

Taken together, the geochemical composition of Marianas magmas, including Anatahan, shows systematic trends consistent with different proportions of subducted sediment in their mantle source. The mantle beneath the Marianas arc appears to be somewhat more depleted than MORB (others have attributed this to prior melting beneath the back arc basin; Woodhead et al., 1993). The inferred sedimentary end-member is very similar isotopically to the bulk sediment subducting at the Marianas trench, although some trace elements are fractionated during melting (Hf from Nd, and Sm from La). Fluids from the subducting oceanic crust contribute significant Pb and Ba to the mantle source. The amount of sediment added to the Anatahan mantle is 1–3 wt.% (from the various mixing models above), and is at the high end for the Marianas arc. The only isotopic system potentially inconsistent with 1–3% bulk sediment in the Anatahan source is $\delta^{18}\text{O}$. Incorporation of 1–3% of sedi-

ments with a $\delta^{18}\text{O}$ value of $\sim 24\text{‰}$ (Ito and Stern, 1986) would increase the $\delta^{18}\text{O}$ value of a magma by 0.2–0.5‰. This would lead to mafic compositions above the mantle field in Fig. 10, which are not observed.

The mixing constraints for oxygen are different from those for trace elements, however, in that all components (mantle, sediment, and fluid) will have roughly similar oxygen concentrations. Oxygen is most sensitive to the mixing proportions, while trace elements are only dependent on the total mass balance. It would be possible to satisfy all isotopic and trace element systems if the sediment proportion was $<1\%$ (to satisfy oxygen) and simply a factor of 1–3 times more enriched in trace element concentrations. In the prior models, we chose bulk sediment concentrations when possible to keep the mixing models simple, even though it is likely that sedimentary components will be transported in a melt phase which may very well be one to three times enriched in concentration over the bulk sediment. Thus, the mixing calculations performed here, combined with the constraints from $\delta^{18}\text{O}$, indicate that the Anatahan mantle source contains equivalent trace elements to 1–3% bulk sediment, concentrated in a sediment melt that constitutes $<1\%$ of the mantle source.

While 1–3% sediment may sound like a small number, it is important to place this result in the context of the total amount of sediment available. If the entire sedimentary column at the Marianas trench contributes to Marianas magma, this would only constitute 4–8% bulk sediment relative to the mantle melting volume. This calculation uses the mass flux for the subducting Marianas sedimentary column (0.3 Mg/year/cm trench length; Plank and Langmuir, 1998), and the full range in magmatic output rates from Reymer and Schubert (1984) and Dimalanta (2002) for the Marianas arc (29–50 km³/Ma/km), and assumes 2.8 g/cm³ density of the arc crust, and 20% mantle melting to create Mariana basalts. Thus, 1–3% subducted sediment in the Anatahan mantle is roughly one third of the total amount sediment inventory subducted at the trench. Loss of the entire upper pelagic clay section, as is indicated by the high Th/La at Anatahan, would only lead to a small (6%) mass reduction in the total sediment input (because it is a thin layer, 65 m thick, with very high porosity). Nonetheless, because this unit is so enriched in trace

elements, the geochemical mixing models are sensitive to its fate.

6. Conclusions

Very little was known about the geochemical evolution of Anatahan volcano prior to the May 2003 eruption. The recently erupted materials have provided us with an opportunity to learn from this volcano. The May 03 eruptives are neither the most primitive nor most fractionated products for Anatahan, and they are identical to materials erupted from Anatahan in its past. Nonetheless, the May 03 volcanic rocks are more silicic than any other rocks in the modern Mariana Islands, and so they provide a unique window into the evolution of these island-arc magmas. Anatahan andesites and dacites have nearly identical isotopic and incompatible trace element ratios to Anatahan basalts, and so this volcano taps very similar parental magmas, and fractionates in a simple way. Several geochemical tests applied in this study failed to reveal evidence for crustal melting or assimilation in the evolution of Anatahan magmas. Instead, Anatahan appears to evolve mainly by crystal fractionation, and as such provides an excellent natural example of certain petrologic phenomena, such as the point of apatite saturation, trace element partition coefficients, phenocryst equilibria, and liquid lines of descent. The geochemical composition of the Anatahan parent magma also has a unique fingerprint within the Marianas, and appears to derive from a mantle source that includes a significant subducted sedimentary component (equivalent to 1–3% bulk sediment). Some geochemical features of Anatahan indicate that the upper ~50 m of the sedimentary section was lost to the shallow levels of the subduction zone. Nonetheless, as much as one third of the subducted sedimentary section has recycled to the volcano.

Acknowledgements

We would like to thank Mike Cunningham of Americopters for transport to and from Anatahan during both the May 2003 and April 2004 sampling trips, as well as Alison Shaw for exceptional help in

the field. Florencia Meana-Prado, Caitlin Masaric-Johnson, and Louise Bolge provided able analytic assistance. Useful comments from editor J. Pallister as well as reviewers B. Leeman and M. Reagan greatly strengthened this manuscript. This research was funded by NSF OCE 0001897 MARGINS to T. Plank, NSF OCE 0325189 to J. Gill, NSF OCE 0305218 MARGINS to T. Fischer, and NSF OCE 0305248 to D. Hilton.

References

- Abrams, L.J., Pockalny, R.A., Larson, R.L., Kelley, K., 2001. A model for the temporal emplacement of oceanic crust at Hole 801C. *Eos, Trans. Am. Geophys. Union, Fall Meet. Suppl.*, vol. 82.
- Armstrong, J.T., 1995. A package of correction programs for the quantitative electron microbeam S-ray analysis of thick polished material, thin films and particles. *Microbeam Analysis* 4, 177–200.
- Bartolini, A., Larson, R.L., 2001. Pacific microplate and the Pangea supercontinent in the early to middle Jurassic. *Geology* 29, 735–738.
- Bryant, C.J., Arculus, R.J., Eggins, S.M., 1999. Laser ablation-inductively coupled plasma-mass spectrometry and tephra: a new approach to understanding arc-magma genesis. *Geology* 27 (12), 1119–1122.
- Bryant, C.J., Arculus, R.J., Eggins, S.M., 2003. The geochemical evolution of the Izu–Bonin arc system: a perspective from tephra recovered by deep-sea drilling. *Geochemistry, Geophysics, Geosystems* 4 (11). doi:10.1029/2002GC000427.
- Castillo, P.R., Floyd, P.A., France-Lanord, C., Alt, J.C., 1992. Data report: summary of geochemical data for Leg 129 igneous rocks. In: Larson, R.L., Lancelot, Y., et al., (Eds.), *Proc. ODP, Sci. Results, Ocean Drilling Program, College Station, TX, Leg 129*, pp. 653–670.
- Chauvel, C., Blichert-Toft, J., 2001. A hafnium isotope and trace element perspective on melting of the depleted mantle. *Earth and Planetary Science Letters* 190 (3–4), 137–151.
- Cooper, K.M., Eiler, J.M., Asimow, P.D., Langmuir, C.H., 2004. Oxygen isotope evidence for the origin of enriched mantle beneath the mid-Atlantic ridge. *Earth and Planetary Science Letters* 220 (3–4), 297–316.
- Cosca, M.A., Arculus, R.J., Pearce, J.A., Mitchell, J.G., 1998. $^{40}\text{Ar}/^{39}\text{Ar}$ and K–Ar geochronological age constraints for the inception and early evolution of the Izu–Bonin–Mariana arc system. *Island Arc* 7 (3), 579–595.
- Davidson, J.P., 1987. Crustal contamination versus subduction zone enrichment: examples from the Lesser Antilles and implications for mantle source compositions of island arc volcanic rocks. *Geochimica et Cosmochimica Acta* 51, 2185–2198.
- de Moor, J.M., Fischer, T.P., Hilton, D.R., Hauri, E., Jaffe, L.A., Camacho, J.T., 2005. Degassing at Anatahan volcano during the May 2003 eruption: implications from petrology, ash leachates,

- and SO₂ emissions. *Journal of Volcanology and Geothermal Research* 146, 117–138 (this issue).
- Dimalanta, C., 2002. New rates of western Pacific island arc magmatism from seismic and gravity data. *Earth and Planetary Science Letters* 202, 105–115.
- Dixon, T.H., Batiza, R., 1979. Petrology and chemistry of recent lavas in the northern Marianas; implications for the origin of island arc basalts. *Contributions to Mineralogy and Petrology* 70 (2), 167–181.
- Eiler, J.M., 2001. Oxygen isotope variations of basaltic lavas and upper mantle rocks. *Stable Isotope Geochemistry* 43, 319–364.
- Eiler, J.M., Crawford, A., Elliott, T., Farley, K.A., Valley, J.W., Stolper, E.M., 2000. Oxygen isotope geochemistry of oceanic-arc lavas. *Journal of Petrology* 41 (2), 229–256.
- Elliott, T.R., 2003. Tracers of the slab. In: Eiler, J. (Ed.), *Inside the Subduction Factory*. American Geophysical Union Monograph, vol. 138. American Geophysical Union, Washington, DC, pp. 23–45.
- Elliott, T., Plank, T., Zindler, A., White, W., Bourdon, B., 1997. Element transport from slab to volcanic front at the Mariana arc. *Journal of Geophysical Research* 102 (B7), 14991–15019.
- Evans, O.C., Hanson, G.N., 1993. Accessory-mineral fractionation of rare-earth element (REE) abundances in granitoid rocks. *Chemical Geology* 110, 69–93.
- Fisk, M., Kelley, K.A., 2002. Probing the Pacific's oldest MORB glass: mantle chemistry and melting conditions during the birth of the Pacific plate. *Earth and Planetary Science Letters* 202, 741–752.
- Ghiorso, M.S., Hirschmann, M.M., Reiners, P.W., Kress III, V.C., 2002. The pMELTS: a revision of MELTS for improved calculation of phase relations and major element partitioning related to partial melting of the mantle to 3 GPa. *Geochemistry, Geophysics, Geosystems* 3 (5). doi:10.1029/2001GC000217.
- Gill, J.B., 1981. *Orogenic Andesites and Plate Tectonics*. Springer-Verlag, New York, 390 pp.
- Gravatt, D.R., 1997. Magma genesis and evolution processes on the islands of Grenada and St. Lucia, Lesser Antilles. MS Thesis, Cornell University, Ithaca, NY.
- Grove, T.L., Elkins-Tanton, L.T., Panman, S.W., Chatterjee, N., Muntener, O., Gaetani, G.A., 2003. Fractional crystallization and mantle-melting controls on calc-alkaline differentiation trends. *Contributions to Mineralogy and Petrology* 145 (5), 515–533.
- Hermann, J., 2002. Allanite: thorium and light rare earth element carrier in subducted crust. *Chemical Geology* 192, 289–306.
- Hildreth, W., Moorbath, S., 1988. Crustal contributions to arc magmatism in the Andes of central Chile. *Contributions to Mineralogy and Petrology* 98, 455–489.
- Hofmann, A.W., Jochum, K.P., Seufert, M., White, W.M., 1986. Nb and Pb in oceanic basalts; new constraints on mantle evolution. *Earth and Planetary Science Letters* 79, 33–45.
- Hole, M.J., Saunders, A.D., Marriner, G.F., Tarney, J., 1984. Subduction of pelagic sediments; implications for the origin of Ce-anomalous basalts from the Mariana Islands. *Journal of the Geological Society (London)* 141 (3), 453–472.
- Ito, E., Stern, R.J., 1986. Oxygen isotopic and strontium isotopic investigations of subduction zone volcanism—the case of the Volcano arc and the Marianas Island arc. *Earth and Planetary Science Letters* 76 (3–4), 312–320.
- Ito, E., Stern, R.J., Douthitt, C., 2003. Insights into operation of the subduction factory from the oxygen isotopic values of the southern Izu–Bonin–Mariana Arc. *Island Arc* 12 (4), 383–397.
- Johnson, M.C., Plank, T., 1999. Dehydration and melting experiments constrain the fate of subducted sediments. *Geochemistry, Geophysics, Geosystems* 1. doi:10.1029/1999GC000014.
- Kay, R.W., Sun, S.-S., Lee-Hu, C.-N., 1978. Pb and Sr isotopes in volcanic rocks from the Aleutian Islands and Pribilof Islands, Alaska. *Geochimica et Cosmochimica Acta* 42, 263–273.
- Kelemen, P.B., Hanghoj, K., Greene, A.R., 2003. One view of the geochemistry of subduction-related magmatic arcs, with an emphasis on primitive andesite and lower crust. In: Rudnick, R.L., Holland, H.D., Turekian, K.K. (Eds.), *The Crust, Treatise on Geochemistry*, vol. 3. Elsevier-Perгамon, Oxford, pp. 593–659.
- Kelley, K.A., 2003. Trench inputs and arc outputs in the Mariana–Izu–Bonin subduction factory. PhD thesis, Boston University, Boston, MA.
- Kelley, K.A., Plank, T., Ludden, J., Staudigel, H., 2003. Composition of altered oceanic crust at ODP Sites 801 and 1149. *Geochemistry, Geophysics, Geosystems* 4 (6). doi:10.1029/2002GC000435.
- Kersting, A.B., Arculus, R.J., Gust, D.A., 1996. Lithospheric contributions to arc magmatism: isotope variations along strike in volcanoes of Honshu, Japan. *Science* 272, 1464–1468.
- Koppers, A.A.P., Staudigal, H., Pringle, M.S., Wijbrans, J.R., 2003a. Short-lived and discontinuous intraplate volcanism in the South Pacific: hot spots or extensional volcanism? *Geochemistry, Geophysics, Geosystems* 4. doi:10.1029/2003GC000533.
- Koppers, A.A.P., Staudigal, H., Duncan, R.A., 2003b. High-resolution ⁴⁰Ar/³⁹Ar dating of the oldest oceanic basement basalts in the western Pacific basin. *Geochemistry, Geophysics, Geosystems* 4. doi:10.1029/2003GC000574.
- Lancelot, Y., Larson, R.L., et al., 1990. Proc. ODP, Init. Repts., Ocean Drilling Program, College Station, TX, Leg 129.
- Larson, E.E., Reynolds, R.L., et al., 1975. Major-element petrochemistry of some extrusive rocks from the volcanically active Mariana Islands. *Bulletin Volcanologique* 38 (2), 361–377.
- Lee, J., Stern, R.J., Bloomer, S.H., 1995. Forty million years of magmatic evolution in the Mariana arc: the tephra glass record. *Journal of Geophysical Research* 100 (B9), 17671–17687.
- Lin, P.N., Stern, R.J., Morris, J., Bloomer, S.H., 1990. Nd- and Sr-isotopic composition of lavas from the northern Mariana and southern Volcano Arcs: implications for the origin of island arc melts. *Contributions to Mineralogy and Petrology* 105, 381–392.
- Lundstrom, C.C., Shaw, H.F., Ryerson, F.J., Williams, Q., Gill, J., 1998. Crystal chemical control of clinopyroxene-melt partitioning in the Di–Ab–An system; implications for elemental fractionations in the depleted mantle. *Geochimica et Cosmochimica Acta* 62 (16), 2849–2862.

- Manton, W.I., 1988. Separation of Pb from young zircons by single-bead ion exchange. *Chemical Geology* 73, 147–152.
- McDonough, W.F., Sun, S.-S., 1995. The composition of the Earth. *Chemical Geology* 120, 223–253.
- Meijer, A., 1976. Pb and Sr isotopic data bearing on the origin of volcanic rocks from the Mariana island–arc system. *Geological Society of America Bulletin* 87, 1358–1369.
- Miller, D.M., Goldstein, S.L., Langmuir, C.H., 1994. Cerium lead and lead-isotope ratios in arc magmas and the enrichment of lead in the continents. *Nature* 368 (6471), 514–520.
- Miyashiro, A., 1974. Volcanic rock series in island arcs and active continental margins. *American Journal of Science* 274, 321–355.
- Moore, R.B., Trusdell, F.A., 1993. Geologic map of Alamagan Volcano, Northern Mariana Islands. *SGS Map* 1-2408.
- Moore, R.B., Koyanagi, R.Y., Sako, M.K., Trusdell, F.A., Kojima, G., Ellorda, R.L., Zane, S., 1991. Volcanologic investigations in the Commonwealth of the Northern Mariana Islands, September–October 1990. *US Geological Survey Open-File Report* 91-320.
- Moore, R.B., Koyanagi, R.Y., Sako, M.K., Trusdell, F.A., Ellorda, R.L., Kojima, G., 1993. Volcanologic investigations in the Commonwealth of the Northern Mariana Islands, May 1992. *US Geological Survey Open-File Report* 93-541.
- Morris, J.D., Hart, S.R., 1983. Isotopic and incompatible element constraints on the genesis of island arc volcanics from Cold Bay and Amak Island, Aleutians, and implications for mantle structure. *Geochimica et Cosmochimica Acta* 47, 2015–2030.
- Münker, C., Weyer, S., Sherer, E., Mezger, K., 2001. Separation of high field strength elements (Nb, Ta, Zr, Hf) and Lu from rock samples for MC-ICPMS measurements. *Geochemistry, Geophysics, Geosystems* 2. doi:10.1029/2001GC000183.
- Nakamura, N., 1974. Determination of REE, Ba, Fe, Mg, Na, and K in carbonaceous and ordinary chondrites. *Geochimica et Cosmochimica Acta* 38, 757–775.
- Pallister, J.S., Trusdell, F.A., Brownfield, I.K., Siems, D.F., Budahn, J.R., Sutley, S.F., 2005. The 2003 phreatomagmatic eruptions of Anatahan volcanotextural and petrologic features of deposits at an emergent island volcano. *Journal of Volcanology and Geothermal Research* 146, 208–225 (this issue).
- Pearce, J., Kempton, P., Nowell, G., Noble, S., 1999. Hf–Nd element and isotope perspective on the nature and provenance of mantle and subduction components in western Pacific arc–basin systems. *Journal of Petrology* 40, 1579–1611.
- Piccoli, P.M., Candela, P.A., 2002. Apatite in igneous systems. In: Kohn, M.J., Rakovan, J., Hughes, J.M. (Eds.), *Phosphates: Geochemical, Geobiological, and Materials Importance*. *Reviews in Mineralogy and Geochemistry*, vol. 48. Mineralogical Society of America.
- Plank, T., in press. Constraints from Th/La sediment recycling at subduction zones and the evolution of the continents. *Journal of Petrology*. doi:10.1093/petrology/egi005.
- Plank, T., Langmuir, C.H., 1993. Tracing trace elements from sediment to volcanic output at subduction zones. *Nature* 362, 739–742.
- Plank, T., Langmuir, C.H., 1998. The chemical composition of subducting sediment and its consequences for the crust and mantle. *Chemical Geology* 145, 325–394.
- Pockalny, R.A., Larson, R.L., 2003. Implications for crustal accretion at fast spreading ridges from observations in Jurassic oceanic crust in the western Pacific. *Geochemistry, Geophysics, Geosystems* 4. doi:10.1029/2001GC000274.
- Reagan, M., Tepley, F.J. III, Gill, J.B., Wortel, M., Hartman, B., 2005. Rapid time scales of basalt to andesite differentiation at Anatahan volcano, Mariana Islands. *Journal of Volcanology and Geothermal Research* 146, 171–183 (this issue).
- Reymer, A., Schubert, G., 1984. Phanerozoic addition rates to the continental crust and crustal growth. *Tectonics* 3, 63–77.
- Rowland, S.K., Lockwood, J.P., Trusdell, F.A., Moore, R.B., Sako, M.K., Koyanagi, R.Y., Kojima, G., 2005. Anatahan, Northern Mariana Islands: reconnaissance geological observations during and after the volcanic crisis of spring 1990, and monitoring prior to the May 2003 eruption. *Journal of Volcanology and Geothermal Research* 146, 26–59 (this issue).
- Salter, V.J.M., Stracke, A., 2004. Composition of the depleted mantle. *Geochemistry, Geophysics, Geosystems* 5. doi:10.1029/2003GC000597.
- Sharp, Z.D., 1990. A laser-based microanalytical method for the in situ determination of oxygen isotope ratios of silicates and oxides. *Geochimica et Cosmochimica Acta* 54, 1353–1357.
- Stern, R.J., Fouch, M.J., Klemperer, S.L., 2003. An overview of the Izu–Bonin–Mariana subduction factory. In: *Inside the Subduction Factory*. *Geophysical Monograph*. American Geophysical Union, vol. 138, pp. 175–222.
- Sun, S.-S., 1980. Lead isotopic study of young volcanic rocks from id-oceanic ridges, oceanic islands, and island arcs. *Philosophical Transactions of the Royal Society of London*. A 297, 409–445.
- Taggart, J.E. (Ed.), 2002. *Analytical Methods for Chemical Analysis of Geologic and Other Materials*. *US Geological Survey Open-File Report*, vol. 2-223.
- Taggart, J.E., Lindsey Jr., J.R., Vivit, D.V., Bartel, A.J., Stewart, K.C., 2002. Analysis of geologic materials by wavelength-dispersive X-ray fluorescence spectrometry. In: Baedeker, P.A. (Ed.), *Methods for Geochemical Analyses*. *U.S. Geological Survey Professional Paper*, vol. 1770.
- Tamura, Y., Tatsumi, Y., Zhao, D.P., Kido, Y., Shukuno, H., 2002. Hot fingers in the mantle wedge: new insights into magma genesis in subduction zones. *Earth and Planetary Science Letters* 197 (1–2), 105–116.
- Tatsumi, Y., Eggins, S., 1995. *Subduction Zone Magmatism*. Blackwell Science, London, 211 pp.
- Tatsumoto, M., Knight, R., 1969. Isotopic composition of lead in volcanic rocks from central Honshu—with regard to basalt genesis. *Geochemistry* 3, 53–86.
- Taylor, H., Sheppard, S.M.F., 1986. Igneous rocks: I. Processes of isotopic fractionation and isotope systematics. In: Valley, J.W., Taylor, H.P., O’Neil, J.R. (Eds.), *Stable Isotopes in High Temperature Geological Processes*. *Reviews in Mineralogy*. Mineralogical Society of America.

- Tera, F., Brown, L.D., Morris, J.D., Sacks, S.I., Klein, J., Middleton, R., 1986. Sediment incorporation in island-arc magmas: inferences from ^{10}Be . *Geochimica et Cosmochimica Acta* 50, 535–550.
- Trusdell, F.A., Moore, R.B., Sako, M., White, R.A., Koyanagi, S.K., Chong, R., Camacho, J.T., 2005. The 2003 eruption of Anatahan Volcano, Commonwealth of the Northern Mariana Islands: chronology, volcanology, and deformation. *Journal of Volcanology and Geothermal Research* 146, 184–207 (this issue).
- Turner, S., Hawkesworth, C., van Calsteren, P., Heath, E., Macdonald, R., Black, S., 1996. U-series isotopes and destructive plate margin magma genesis in the Lesser Antilles. *Earth and Planetary Science Letters* 142, 191–207.
- Valley, J.W., Kitchen, N., Kohn, M.J., Niendorff, C.R., Spicuzza, M.J., 1995. Strategies for high precision oxygen isotope analysis by laser fluorination. *Geochimica et Cosmochimica Acta* 59, 5223–5231.
- Vervoort, J.D., Patchett, P.J., Blichert-Toft, J., Albarède, F., 1999. Relationships between Lu–Hf and Sm–Nd isotopic systems in the global sedimentary system. *Earth and Planetary Science Letters* 168, 79–99.
- Watson, E.B., Harrison, T.M., 1984. Accessory minerals and the geochemical evolution of crustal magmatic systems: a summary and prospectus of experimental approaches. *Physics of the Earth and Planetary Interiors* 35, 19–30.
- Wood, B.J., Blundy, J.D., 1997. A predictive model for rare earth element partitioning between clinopyroxene and anhydrous silicate melt. *Contributions to Mineralogy and Petrology* 129, 166–181.
- Woodhead, J.D., 1987. Geochemistry of volcanic rocks from the Northern Mariana Islands, Western Pacific. PhD thesis, University of Oxford, Oxford, UK.
- Woodhead, J.D., 1988. The origin of geochemical variations in Mariana lavas: a general model for petrogenesis in intra-oceanic island arcs? *Journal of Petrology* 29, 805–830.
- Woodhead, J.D., 1989. Geochemistry of the Mariana Arc (Western Pacific): source composition and processes. *Chemical Geology* 76 (1–2), 1–24.
- Woodhead, J.D., 2002. A simple method for obtaining highly accurate Pb isotopic data by MC-ICP-MS. *Journal of Analytical Atomic Spectrometry* 17, 1381–1385.
- Woodhead, J.D., Fraser, D.G., 1985. Pb, Sr, and ^{10}Be isotopic studies of volcanic rocks from the Northern Mariana Islands. Implications for magma genesis and crustal recycling in the western Pacific. *Geochimica et Cosmochimica Acta* 49, 1925–1930.
- Woodhead, J.D., Eggins, S., Gamble, J., 1993. High field strength and transition element systematics in island arc and back-arc basin basalts: evidence for multi-phase melt extraction and a depleted mantle wedge. *Earth and Planetary Science Letters* 114, 491–504.
- Woodhead, J.D., Volker, F., McCulloch, M.T., 1995. Routine Pb isotope determinations using a ^{207}Pb – ^{204}Pb double spike: a long term assessment of analytical precision and accuracy. *The Analyst* 120, 35–39.
- Woodhead, J.D., Hergt, J.M., Davidson, J.P., Eggins, S.M., 2001. Hafnium isotope evidence for ‘conservative’ element mobility during subduction zone processes. *Earth and Planetary Science Letters* 192, 331–346.
- Woodhead, J.D., Stern, R.J., Pearce, J.A., 2001. Further Hf-isotope constraints on element mobility within subduction zones. SOTA Conference Abstract.